

Biological Feature Vector Modulation By First and Second Messenger Pathways

James Peterson

Department of Mathematical Sciences

Clemson University

email: `petersj@clemson.edu`

October 25, 2005

Abstract

We present an abstract model of the output of an excitable cell in which a generic Hodgkin - Huxley class action potential is replaced by a low dimensional biologically based feature vector or BFV. The voltage pulse that arrives at the axon hillock of the neuron model must then modulate the BFV output in accordance to first and second messenger effects seen in the neural element's input and cell body regions. We derive algorithms from first principles for the combination of two BFV's, in a useful biological manner, which are used in input side computations. We also indicate how first and second messenger inputs can modulate the components of the BFV in efficient manner. These algorithms are therefore part of a model which consists of three critical components: first, a model of dendritic processing and soma processing that requires an abstract view of second messenger processing; second, a detailed algorithm which determines what voltage is presented to the axon hillock of the neuron based upon the first and second messenger influences presented in the inputs and third; a suite of mechanisms which determine the shape of the resulting action potential which the neuron emits. These abstractions have been carefully designed to permit the neuron model to be plastic at both the hardware and software levels. Hence, the design details of their implementation within an asynchronous programming protocol on a variety of computer networks have always been part of the development process.

1 Introduction:

There has now been a substantial body of work, summarized in (Prete (8) 2004) on the possibility of cognitive states arising in very small brain animals. The current research with small brain animals such as certain spiders (Prete (8, Chap. 1) 2004), praying mantis's (Prete (8, Chap. 3) 2004) and frogs (Prete (8, Chap. 4) 2004) clearly indicates that the cognitive capabilities of so-called simple nervous systems are far greater than we originally thought. We infer

from this that there does not seem to be a need to assume that only the full complexity of the human brain is required to develop a useful model of cognition and consciousness. As a starting position in the study of cognition, based on the studies above, we posit that cognition and consciousness inevitably arise from the following building blocks.

- The animal lives in environment where sensory input is varied and ambiguous. A collection of nested and potentially overlapping filters that assign low dimensional information vectors to raw input gives what is called a *sense* S . It is important that the animal have a finite collection of senses S_1, \dots, S_N which process the raw inputs of the world.
- The animal's survival does not depend on any fixed strategy. Hence, sensory information from sensors S_1, \dots, S_N must be fused to form higher level precepts. Survival decisions must be multi-criteria in nature with difficult to define optimal values. This implies the existence of neural circuitry that is hierarchically organized. Raw information flows into separate modules of neural tissue through the primary sense filters. These modules, call them sensory cortex, are connected to the outside world. The sensory cortex then connects to additional modules which are not connected to external stimulation. We will call these additional modules associative cortex.
- The associative cortex modules can be modulated by neurotransmitter inputs from another circuit module. We can call this central modulation circuitry the central core.
- The three elements above form a dynamical system. The central core innervates the associative and sensory cortex and the associative cortex feeds back to the central core and the sensory cortex.

We can summarize these ideas graphically in Figure 1. In most animals studied, the midcore region is given the name of *thalamus* from the relevant human structure and the reentrant connections are called the *thalamo - cortical loop*. Homologous structures to the thalamo - cortical loop appear to be present in birds and certain insects and other species.

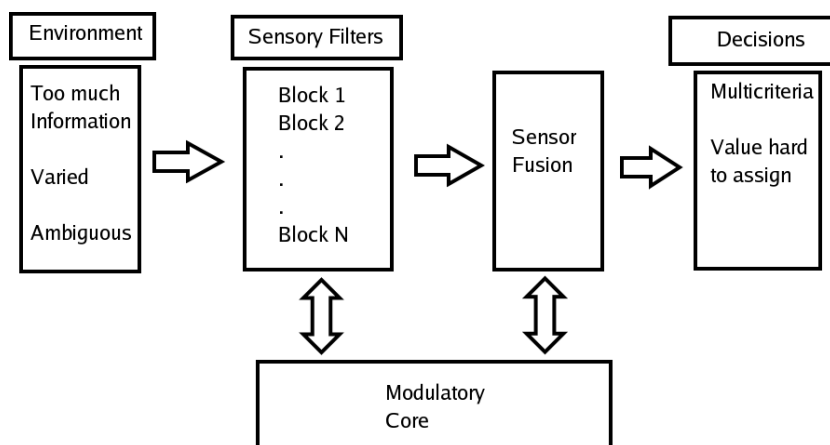


Figure 1: Basic Cognitive Circuitry

We mention all of the above material as background to motivate the material we set forth in this paper. In order to eventually say something quantitative about what minimal systems and interactions are required to develop consciousness and cognition, we need a model of the abstract information processing of an excitable nerve cell with hardware/ software plasticity. We have been developing

such a model and it consists of three critical components: first, a model of dendritic processing and soma processing that requires an abstract view of second messenger processing; second, a detailed algorithm which determines what voltage is presented to the axon hillock of the neuron based upon the first and second messenger influences presented in the inputs and third; a suite of mechanisms which determine the shape of the resulting action potential which the neuron emits. In addition, we replace the action potential by a low dimensional feature vector to ameliorate the computational burdens. The arguments detailing this model are long and involved and in this paper, we will only discuss modulation algorithms for the BFV outputs of the neuron model. The discussion of the second messenger processing algorithms are detailed in (Peterson (5) 2005) and our complete working notes can be found in (Peterson (6) 2005) . However, our hope is that this long introduction places our efforts within a larger scale framework explaining their purpose.

2 An Excitable Cell Model

We begin by discussing the basics of information processing in a typical neuron or excitable nerve cell (Hall (1, see 1992) . Our basic model consists of the following structural elements: A neuron which consists of a *dendritic tree* (which collects sensory stimuli and sums this information in a temporally and spatially dependent way), a cell body (called the *soma*) and an output fiber (called the *axon*). Individual dendrites of the dendritic tree and the axon are all modeled as cylinders of some radius a whose length ℓ is very long compared to this radius and whose walls are made of a bilipid membrane. The inside of each cylinder consists of an intracellular fluid and we think of the cylinder as lying in a bath of extracellular fluid. So for many practical reasons, we can model a dendritic or axonal fiber as two concentric cylinders; an inner one of radius a (this is the actual dendrite or axon) and an outer one with the extracellular fluid contained in the space between the inner and outer membranes.

The potential difference across the inner membrane is essentially due to a balance between the electromotive force generated by charge imbalance, the driving force generated by charge concentration differences in various ions and osmotic pressures that arise from concentration differences in water molecules on either side of the membrane. Roughly speaking, the ions of importance in our simplified model are the potassium K^+ , sodium Na^+ and chloride Cl^- ions. The equilibrium potential across the inner membrane is about -70 millivolts and when the membrane potential is driven above this rest value, we say the membrane is *depolarized* and when it is driven below the rest potential, we say the membrane is *hyperpolarized*. The axon of one neuron interacts with the dendrite of another neuron via a site called a *synapse*. The synapse is physically separated into two parts: the *presynaptic* side (the side the axon is on) and the *postsynaptic* side (the side the dendrite is on). There is an actual physical gap, the *synaptic cleft*, between the two parts of the synapse. This cleft is filled with extracellular fluid.

If there is a rapid depolarization of the presynaptic site, a chain of events is initialized which culminates in the release of specialized molecules called *neurotransmitters* into the synaptic cleft. There are pores embedded in the postsynaptic membrane whose opening and closing are dependent on the potential across the membrane that are called

voltage-dependent gates. In addition, the gates generally allow the passage of a specific ion; so for example, there are sodium, potassium and chloride gates. The released neurotransmitters bind with the sites specific for the Na^+ ion. Such sites are called *receptors*. Once bound, Na^+ ions begin to flow across the membrane into the fiber at a greater rate than before. This influx of positive ions begins to drive the membrane potential above the rest value; that is, the membrane begins to depolarize. The flow of ions across the membrane is measured in gross terms by what are called *conductances*. Conductance has the units of reciprocal ohms; hence, high conductance implies high current flow per unit voltage. Thus the conductance of a gate is a good way to measure its flow. We can say that as the membrane begins to depolarize, the sodium conductance, g_{Na} , begins to increase. This further depolarizes the membrane. However, the depolarization is self-limited as the depolarization of the membrane also triggers the activation of voltage-dependent gates for the potassium ion, K^+ , which allow potassium ions to flow through the membrane out of the cell. So the increase in the sodium conductance, g_{Na} triggers a delayed increase in potassium conductance, g_K (there are also conductance effects due to chloride ions which we will not mention here). The net effect of these opposite driving forces is the generation of a potential pulse that is fairly localized in both time and space. It is generated at the site of the synaptic contact and then begins to propagate down the dendritic fiber toward the soma. As it propagates, it attenuates in both time and space. We call these voltage pulses *Post Synaptic Pulses* or PSPs.

We can model the soma itself as a small isopotential sphere, small in surface area compared to the surface area of the dendritic system. The possibly attenuated values of the PSPs generated in the dendritic system at various times and places are assumed to propagate without change from any point on the soma body to the initial segment of the axon which is called the *axon hillock*. This is a specialized piece of membrane which generates a large output voltage pulse in the axon by a coordinated rapid increase in g_{Na} and g_K once the axon hillock membrane depolarizes above a critical trigger value. The axon itself is constructed in such a way that this output pulse, called the *action potential*, travels without change throughout the entire axonal fiber. We can model the dendrite fiber reasonably accurately by using what is called the core conductor model. In this model, careful reasoning using Ohm's law and Kirchhoff's laws for current and voltage balance lead to the well-known **core conductor** equation

$$\frac{\partial^2 V_m}{\partial z^2} = (r_i + r_o)K_m(z, t) - r_o K_e(z, t). \quad (1)$$

where r_i and r_o are the resistance per unit length in the inner and outer conductor, K_m is the membrane current from inner to outer conductor per unit length, K_e is the the current per unit length due to external sources applied in a cylindrically symmetric manner and V_m is the membrane potential. It is much more useful to look at this model in terms of transient variables which are perturbations from rest values. We define

$$V_m(z, t) = V_m^0 + v_m(z, t), \quad K_m(z, t) = K_m^0 + k_m(z, t), \quad K_e(z, t) = K_e^0 + k_e(z, t) \quad (2)$$

where the rest values are respectively V_m^0 (membrane rest voltage), K_m^0 (membrane current per length base value) and K_e^0 (injected current per length base value). With the introduction of these transient variables, we are able to model the flow of current across the inner membrane more precisely. We introduce the conductance per length g_m (Siemens/cm or 1/(ohms cm) and capacitance per length c_m (fahrad/cm) of the membrane and note that we can think of a patch of membrane as as simple RC circuit. This leads to the *transient cable* equation

$$\frac{\partial^2 v_m}{\partial z^2} = (r_i + r_o)g_m v_m(z, t) + (r_i + r_o)c_m \frac{\partial v_m}{\partial t} - r_o k_e(z, t). \quad (3)$$

If we write the transient cable equation into an appropriate scaled form, we gain great insight into how membrane voltages propagate in time and space relative to what may be called fundamental scales. Define $\tau_M = \frac{c_m}{g_m}$ and $\lambda_C = \frac{1}{\sqrt{(r_i + r_o)g_m}}$. Note that τ_M , the fundamental time constant, is independent of the geometry of the cable and depends only on dendritic fiber characteristics. This constant determines how quickly a membrane potential decays to one half on its initial value). The constant λ_C is dependent on the geometry of the cable fiber and it can be shown it is the fundamental space constant of the system for the membrane potential decays to one half of its value within this distance along the cable fiber. The space constant can be shown to have units of cm.

The Thévenin equivalent conductance, G_∞ , is then defined to be $G_\infty = \lambda_C g_m$. For most biologically plausible situations, the outer conductor resistance per unit length is very small in comparison to the inner conductor's resistance per unit length. Hence, $r_i \gg r_o$ and $G_\infty = \sqrt{\frac{g_m}{r_i}}$. It follows that $r_i + r_o = \frac{1}{\lambda_C^2 g_m}$ and hence, we can rewrite the transient cable equation as

$$\lambda_C^2 \frac{\partial^2 v_m}{\partial z^2} = v_m + \tau_M \frac{\partial v_m}{\partial t} - r_o \lambda_C^2 k_e. \quad (4)$$

We can convert this into length and time scales based on the fundamental length λ_C and time τ_M . Define the scaled length λ by $\lambda \lambda_C = z$ and the scaled time by $\tau \tau_M = t$. Then it follows that defining $\hat{v}_m(\lambda, \tau) = v_m(\lambda \lambda_C, \tau \tau_M)$, we find

$$\frac{\partial^2 \hat{v}_m}{\partial \lambda^2} = v_m + \frac{\partial \hat{v}_m}{\partial \tau} - r_o \lambda_C^2 k_e(\lambda \lambda_C, \tau \tau_M). \quad (5)$$

2.1 The Ball and Stick Model:

We can now extend our model to the *ball and stick* neuron model which consists of an isopotential sphere (the soma) coupled to a single dendritic fiber input line. We model the soma as a simple parallel resistance/ capacitance network and the dendrite as a finite length cable as previously discussed using scaled length and time It is then possible to show,

with a reasonable zero-rate left end cap condition, the appropriate boundary condition at $\lambda = 0$ is given by

$$\rho \frac{\partial \hat{v}_m}{\partial \lambda}(0, \tau) = \tanh(L) \left[\hat{v}_m(0, \tau) + \frac{\partial \hat{v}_m}{\partial \tau}(0, \tau) \right], \quad (6)$$

where we introduce the fundamental ratio $\rho = \frac{G_D}{G_S}$, the ratio of the dendritic conductance to soma conductance. The full system to solve is therefore:

$$\frac{\partial^2 \hat{v}_m}{\partial \lambda^2} = \hat{v}_m + \frac{\partial \hat{v}_m}{\partial \tau}, \quad 0 \leq z \leq \ell, \quad t \geq 0. \quad (7)$$

$$\frac{\partial \hat{v}_m}{\partial \lambda}(L, \tau) = 0, \quad (8)$$

$$\rho \frac{\partial \hat{v}_m}{\partial \lambda}(0, \tau) = \tanh(L) \left[\hat{v}_m(0, \tau) + \frac{\partial \hat{v}_m}{\partial \tau}(0, \tau) \right]. \quad (9)$$

Applying the technique of separation of variables, $\hat{v}_m(\lambda, \tau) = u(\lambda)w(\tau)$ leads to the system

$$u''(\lambda)w(\tau) = u(\lambda)w(\tau) + u(\lambda)w'(\tau)$$

$$\rho u'(0)w(\tau) = \tanh(L) (u(0)w(\tau) + u(0)w'(\tau))$$

$$u'(L)w(\tau) = 0$$

This leads to the ratio equation $\frac{u''(\lambda)}{u(\lambda)} = \frac{w'(\tau)}{w(\tau)}$. Since these ratios hold for all τ and λ , they must equal a common constant β which is called the separation of variables constant. Thus, we have

$$\frac{d^2 u}{d\lambda^2} = (1 + \beta)u, \quad 0 \leq \lambda \leq L, \quad (10)$$

$$\frac{dw}{d\tau} = \beta w, \quad \tau \geq 0. \quad (11)$$

The boundary conditions then become

$$u'(L) = 0 \quad \rho u'(0) - \tanh(L)u(0) = 0.$$

The only case where we can have non trivial solutions to Equation 10 occur when $1 + \beta = -\alpha^2$ for some constant α . The general solution to Equation 10 is then of the form $A \cos(\alpha\lambda) + B \sin(\alpha\lambda)$. To satisfy the boundary conditions,

we find A and B must be chosen to satisfy the system

$$\begin{aligned} -\alpha^2 \tanh(L)A + \rho\alpha B &= 0 \\ -\alpha \sin(\alpha L) + \alpha \cos(\alpha L) &= 0 \end{aligned}$$

A non trivial solution requires that the determinant of the system be nonzero. This implies α must satisfy the transcendental equation

$$\tan(\alpha L) = -\alpha \frac{\tanh(L)}{\rho}, = -k(\alpha L), \quad (12)$$

where $k = \frac{\tanh(L)}{\rho L}$. The values of α that satisfy Equation 12 give us the eigenvalue of our original problem, $\beta = -1 - \alpha^2$. The eigenvalues of our system can be determined by the solution of the transcendental equation 12. It can be shown that the eigenvalues form a monotonically increasing sequence starting with $\alpha_0 = 0$ and with the values α_n approaching asymptotically the values $\frac{2n-1}{2} \pi$. Hence, there are a countable number of eigenvalues of the form $\beta_n = -1 - \alpha_n^2$ leading to a general solution of the form

$$\hat{v}_m^n(\lambda, \tau) = A_n \cos(\alpha_n \lambda) e^{-(1+\alpha_n^2)\tau}. \quad (13)$$

Hence, this system has the eigenvalue/ eigenfunction pairs given by α_n (the solution to the transcendental equation 12) and $\cos[\alpha_n(L - \lambda)]$. These eigenfunctions are **not** mutually orthogonal in the L^2 inner product (this system is not a Sturm-Liouville system). In fact, we can show that for $n \neq m$,

$$\int_0^L \cos[\alpha_n(L - \lambda)] \cos[\alpha_m(L - \lambda)] = \frac{\sin((\alpha_n + \alpha_m)L)}{\alpha_n + \alpha_m} + \frac{\sin((\alpha_n - \alpha_m)L)}{\alpha_n - \alpha_m}$$

Since $\lim \alpha_n = \frac{(2n-1)\pi}{2}$, we see there is an integer Q so that

$$\int_0^L \cos[\alpha_n(L - \lambda)] \cos[\alpha_m(L - \lambda)] \approx 0$$

if n and m exceed Q . Thus, as usual, we expect the most general solution is given by

$$\hat{v}_m(\lambda, \tau) = A_0 e^{-\tau} + \sum_{n=1}^Q A_n \cos(\alpha_n(L - \lambda))e^{-(1+\alpha_n^2)\tau} + \sum_{n=Q+1}^{\infty} A_n \cos(\alpha_n(L - \lambda))e^{-(1+\alpha_n^2)\tau} \quad (14)$$

Since the spatial eigenfunction are approximately orthogonal, the computation of the coefficients A_n for $n > Q$ can be handled with a straightforward inner product calculation. The calculation of the first Q coefficients must be handled as a linear algebra problem.

3 The Basic Hodgkin - Huxley Model:

A realistic description of how the membrane activity contributes to the membrane voltage uses models of ion flow controlled by gates in the membrane. A simple model of this sort is based on work that Hodgkin and Huxley (Hodgkin and Huxley (4) 1952) , (Hodgkin, Hodgkin (2, 3) 1952, 1954) performed in the 1950's. We start by expanding the membrane model to handle potassium, sodium and an all purpose current, called leakage current, using a modification of our original simple electrical circuit model of the membrane. We will think of a gate in the membrane as having an intrinsic resistance and the cell membrane itself as having an intrinsic capacitance. Thus, we expand the single branch of our old circuit model to multiple branches – one for each ion flow we wish to model. The ionic current consists of the portions due to potassium, I_K , sodium, I_{Na} and leakage I_L . The leakage current is due to all other sources of ion flow across the membrane which are not being explicitly modeled. This would include ion pumps; gates for other ions such as Calcium, Chlorine; neurotransmitter activated gates and so forth. We will assume that the leakage current is chosen so that there is no excitable neural activity at equilibrium. The standard Hodgkin - Huxley model of an excitatory neuron, under the voltage clamped protocol is

$$\frac{dV_m}{dt} = \frac{1}{C_m} (I_E - I_K - I_{Na} - I_L). \quad (15)$$

where C_m is membrane capacitance and I_E is an external current I_E . From circuit theory, we know that the charge q across a capacitor is $q = C E$, where C is the capacitance and E is the voltage across the capacitor. Thus, from Ohm's law, we know that for each ion c , we can say $V_c = I_c R_c$ where we label the voltage, current and resistance due to this ion with the subscript c . This implies $I_c = G_c V_c$, where G_c is the reciprocal resistance or conductance of ion c . Hence, we can model all of our ionic currents using a conductance equation of the form above. The conductance is assumed to have the form

$$G_c(V_m, t) = G_0 \mathcal{M}_c^p(V_m, t) \mathcal{H}_c^q(V_m, t),$$

where appropriate powers of p and q are found to match known data for a given ion conductance. We model the leakage current, I_L , as $I_L = G_L (V_m(t) - E_L)$ where the leakage battery voltage, E_L , and the conductance g_L are constants that are data driven. Hence, in terms of current densities, letting g_K , g_{Na} and g_L respectively denote the ion conductances per length, our full model would be

$$C_m \frac{dV_m}{dt} = I_E - G_K(V_m - E_K) - G_{Na}(V_m - E_{Na}) - G_L(V_m - E_L)$$

Hodgkin and Huxley modeled the sodium and potassium gates, from data, as

$$\begin{aligned} G_{Na}(V_m, t) &= G_0^{Na} \mathcal{M}_{Na}^3(V_m, t) \mathcal{H}_{Na}(V_m, t), \\ G_K(V_m, t) &= G_0^K \mathcal{M}_K^4(V_m, t). \end{aligned}$$

where the activation, \mathcal{M}_{ion} , and the inactivation, \mathcal{H}_{ion} , variables satisfy first order kinetics of the form $\tau_x \frac{dx}{dt} = x_\infty - x$, $x_0 = x_0$, where x can be any of the choices \mathcal{M}_{ion} or \mathcal{H}_{ion} . The model is further complicated by the voltage dependence of the critical constant pairs (τ_x, x_∞) and so forth. These parameters are computed at any given voltage by $\tau_x = \frac{1.0}{\alpha_x + \beta_x}$ and $x_\infty = \frac{\alpha_x}{\alpha_x + \beta_x}$. The needed (α, β) pairs for each activation/ inactivation variable are modeled using curve fits to data as sigmoid type nonlinearities.

4 Second Messenger Models

We now look at pathways used by extracellular triggers but very abstractly as we want to design principles by which we can model second messenger effects. Let T_0 denote a second messenger trigger which moves through a port P to create a new trigger T_1 some of which binds to B_1 . A schematic of this is shown in Figure 2.

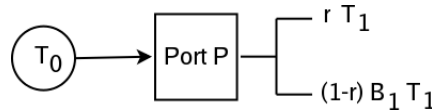
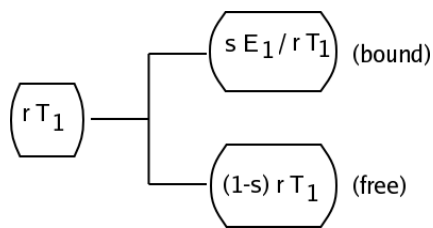


Figure 2: Second Messenger Trigger

In the figure, r is a number between 0 and 1 which represents the fraction of the trigger T_1 which is free in the cytosol. Hence, $100r\%$ of T_1 is free and $100(1-r)$ is bound to B_1 creating a storage complex B_1/T_1 . For our simple model, we assume rT_1 is transported to the nuclear membrane where some of it binds to the enzyme E_1 . Let s in $(0, 1)$ denote the fraction of rT_1 that binds to E_1 . We illustrate this in Figure 3.

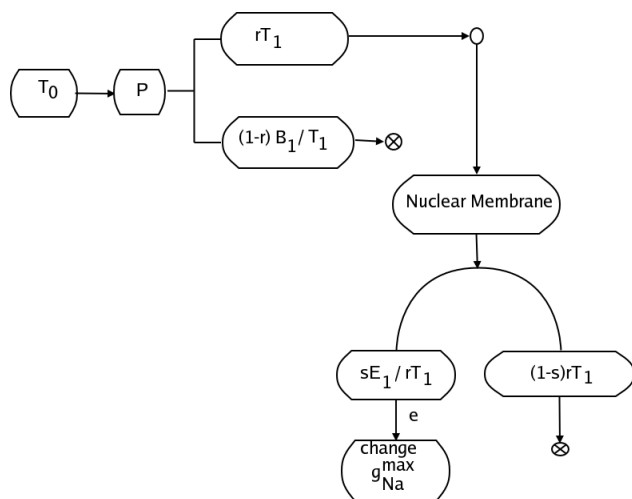
We denote the complex formed by the binding of E_1 and T_1 by E_1/T_1 . From Figure 3, we see that the proportion of T_1 that binds to the genome (DNA) and initiates protein creation $P(T_1)$ is thus srT_1 .

Figure 3: Some T_1 Binds To the Genome

4.1 Generic Second Messenger Triggers:

The protein created, $P(T_1)$, could be many things. Here, let us assume that $P(T_1)$ is a sodium, Na^+ , gate.

Thus, our high level model is



We therefore increase the concentration of Na^+ gates, $[\text{Na}^+]$ thereby creating an increases in the sodium conductance, g_{Na} . The standard Hodgkin - Huxley conductance model (details are in Section 3) is given by

Figure 4: Maximum Sodium Conductance Control Pathway

$$g_{\text{Na}}(t, V) = g_{\text{Na}}^{\text{max}} \mathcal{M}_{\text{Na}}^p(t, v) \mathcal{H}_{\text{Na}}^q(t, V)$$

where t is time and V is membrane voltage. The variables \mathcal{M}_{Na} and \mathcal{H}_{Na} are the activation and inactivation functions for the sodium gate with p and q appropriate positive powers. Finally, $G_{\text{Na}}^{\text{max}}$ is the maximum conductance possible. These models generate \mathcal{M}_{Na} and \mathcal{H}_{Na} values in the range $(0, 1)$ and hence,

$$0 \leq g_{\text{Na}}(t, V) \leq g_{\text{Na}}^{\text{max}}$$

We can model increases in sodium conductances as increases in $g_{\text{Na}}^{\text{max}}$ with efficiency e , where e is a number between 0 and 1. We will not assume all of the $sE_1/rT_1 + \text{DNA}$ to sodium gate reaction is completed. It follows that e is similar to a Michaelson - Mentin kinetics constant. We could also alter activation, \mathcal{M}_{Na} , and/or inactivation, \mathcal{H}_{Na} , as functions of voltage, V in addition to the change in the maximum conductance. However, we are interested in a simple model at present. Our full schematic is then given in Figure 4. We can model the choice process, rT_1 or $(1-r)B_1/T_1$ via a simple sigmoid,

$$f(x) = 0.5 \left(1 + \tanh\left(\frac{x - x_0}{g}\right) \right)$$

where the transition rate at x_0 is $f'(x_0) = \frac{1}{2g}$. Hence, the “gain” of the transition can be adjusted by changing the value of g . We assume g is positive. This function can be interpreted as switching from of “low” state $\mathbf{0}$ to a high state $\mathbf{1}$ at speed $\frac{1}{2g}$. Now the function $h = rf$ provides an output in (r, ∞) . If x is larger than the threshold x_0 , h rapidly transitions to a high state r . On the other hand, if x is below threshold, the output remains near the low state 0 .

We assume the trigger T_0 does not activate the port P unless its concentrations is past some threshold $[T_0]_b$ where $[T_0]_b$ denotes the *base* concentration. Hence, we can model the port activity by

$$h_p([T_0]) = \frac{r}{2} \left(1 + \tanh\left(\frac{[T_0] - [T_0]_b}{g_p}\right) \right)$$

where the two shaping parameters g_p (transition rate) and $[T_0]_b$ (threshold) must be chosen. We can thus model the schematic of Figure 2 as $h_p([T_0])[T_1]_n$ where $[T_1]_n$ is the nominal concentration of the induced trigger T_1 . In a similar way, we let

$$h_e(x) = \frac{s}{2} \left(1 + \tanh\left(\frac{x - x_0}{g_e}\right) \right)$$

Thus, for $x = h_p([T_0])[T_1]_n$, we have h_e is a switch from 0 to s . Note that $0 \leq x \leq r[T_1]_n$ and so if $h_p([T_0])[T_1]_n$ is close to $r[T_1]_n$, h_e is approximately s . Further, if $h_p([T_0])[T_1]_n$ is small, we will have h_e is close to 0 . This suggests a threshold value for h_e of $\frac{r[T_1]_n}{2}$. We conclude

$$h_e(h_p([T_0])[T_1]_n) = \frac{s}{2} \left(1 + \tanh\left(\frac{h_p([T_0])[T_1]_n - \frac{r[T_1]_n}{2}}{g_e}\right) \right)$$

which lies in $[0, s)$. This is the amount of activated T_1 which reaches the genome to create the target protein $P(T_1)$. It follows then that

$$[P(T_1)] = h_e(h_p([T_0])[T_1]_n)[T_1]_n$$

The protein is created with efficiency e and so we model the conversion of $[P(T_1)]$ into a change in g_{Na}^{max} as follows.

Let

$$h_{Na}(x) = \frac{e}{2} \left(1 + \tanh\left(\frac{x - x_0}{g_{Na}}\right) \right)$$

which has output in $[0, e)$. Here, we want to limit how large a change we can achieve in g_{Na}^{max} . Hence, we assume there is an upper limit which is given by $\Delta g_{Na}^{max} = \delta_{Na} g_{Na}^{max}$. Thus, we limit the change in the maximum sodium conductance to some percentage of its baseline value. It follows that $h_{Na}(x)$ is about δ_{Na} if x is sufficiently large and small otherwise. This suggests that x should be $[P(T_1)]$ and since translation to $P(T_1)$ occurs no matter how low $[T_1]$ is, we can use a switch point value of $x_0 = 0$. We conclude

$$h_{Na}([P(T_1)]) = \frac{e}{2} \delta_{Na} g_{Na}^{max} \left(1 + \tanh\left(\frac{[P(T_1)]}{g_{Na}}\right) \right) \quad (16)$$

Our model of the change in maximum sodium conductance is therefore $\Delta g_{Na}^{max} = h_{Na}([P(T_1)])$.

We can thus alter the action potential via a second messenger trigger by allowing

$$g_{Na}(t, V) = (g_{Na}^{max} + h_{Na}([P(T_1)])) \mathcal{M}^p(t, V) \mathcal{H}^q(t, V)$$

for appropriate values of p and q within a standard Hodgkin - Huxley model.

Next, if we assume a modulatory agent acts as a trigger T_0 as described above, we can generate action potential pulses using the standard Hodgkin - Huxley model for a large variety of critical sodium trigger shaping parameters. We label these with a Na to indicate their dependence on the sodium second messenger trigger.

$$[r^{Na}, [T_0]_b^{Na}, g_p^{Na}, s^{Na}, g_e^{Na}, e^{Na}, g_{Na}, \delta_{Na}]'$$

We can follow the procedure outlined in this section for a variety of triggers. We therefore can add a potassium gate trigger with shaping parameters

$$[r^K, [T_0]_b^K, g_p^K, s^K, g_e^K, e^K, g_K, \delta_K]'$$

4.1.1 Concatenated Sigmoid Transitions:

In the previous section, we have found how to handle alterations in g_{Na}^{max} due to a trigger T_0 . We have

$$g_{Na}(t, V) = (g_{Na}^{max} + h_{Na}([P(T_1)])) \mathcal{M}_{Na}^p(t, V) \mathcal{H}_{Na}^q(t, V)$$

where

$$h_{Na}([P(T_1)]) = \frac{e}{2} \delta_{Na} g_{Na}^{max} \left(1 + \tanh\left(\frac{[P(T_1)]}{g_{Na}}\right) \right)$$

with e and δ_{Na} in $(0, 1)$. Denote the transition function $\sigma(x, x_0, g_0)$ by

$$\sigma(x, x_0, g_0) = \frac{1}{2} \left(1 + \tanh\left(\frac{x - x_0}{g_0}\right) \right)$$

We can then write the sodium conductance modification equation more compactly as

$$h_{Na}([P(T_1)]) = e \delta_{Na} g_{Na}^{max} \sigma([P(T_1)], 0, g_{Na}).$$

Using this same notation, we see

$$\begin{aligned} h_p([T - 0]) &= r \sigma([T_0], [T_0]_b, g_p) \\ h_e(h_p([T_0])[T_1]_n) &= s \sigma\left(h_p([T_0])[T_1]_n, \frac{r[T_1]_n}{2}, g_e\right) \\ &= s \sigma\left(r \sigma([T_0], [T_0]_b, g_p)[T_1]_n, \frac{r[T_1]_n}{2}, g_e\right) \end{aligned}$$

Note the concatenation of the sigmoidal processing. Now

$$[P(T_1)] = h_e(h_p([T_0])[T_1]_n) [T_1]_n$$

Thus,

$$[P(T_1)] = s \sigma\left(r \sigma([T_0], [T_0]_b, g_p)[T_1]_n, \frac{r[T_1]_n}{2}, g_e\right) [T_1]_n.$$

Finally,

$$g_{Na}(t, V) = g_{Na}^{max} (1 + e\delta_{Na} \sigma([P(T_1)], 0, g_{Na})) \mathcal{M}_{Na}^p(t, V) \mathcal{H}_{Na}^q(t, V)$$

Implicit in this formula is the *cascade* “ $\sigma(\sigma(\sigma(\dots)))$ ” as $h([P(T_1)], 0, g_{Na})$ uses two concatenated sigmoid calculations itself. We label this as a σ_3 transition and use the notation

$$\begin{array}{ll} \sigma_3([T_0], [T_0]_b, g_p; & \text{inner most sigmoid} \\ r; & \text{scale innermost calculation by } r \\ [T_1]_n; & \text{scale again by } [T_1]_n \\ & \text{this is input to next sigmoid} \\ \frac{r[T_1]_n}{2}, g_e; & \text{offset and gain of next sigmoid} \\ s; & \text{scale results by } s \\ [T_1]_n; & \text{scale again by } [T_1]_n \\ & \text{this is } [P(T_1)] \\ & \text{this is input into last sigmoid} \\ 0, g_{Na}; & \text{offset and gain of last sigmoid} \end{array}$$

Thus, the g_{Na} computation can be written as

$$g_{Na}(t, V) = g_{Na}^{max} \left(1 + e\delta_{Na} \sigma_3([T_0], [T_0]_b, g_p; r; [T_1]_n; \frac{r[T_1]_n}{2}, g_e; s; [T_1]_n; 0, g_{Na}) \right) \mathcal{M}_{Na}^p(t, V) \mathcal{H}_{Na}^q(t, V)$$

This implies a trigger T_0 has associated with it a data vector

$$W_{T_0} = \left[[T_0], [T_0]_b, g_p, r, [T_1]_n, \frac{r[T_1]_n}{2}, g_e, s, [T_1]_n, 0, g_T \right]'$$

where g_T denotes the final gain associated with the third level sigmoidal transition to create the final gate product. We can then rewrite our modulation equation as

$$g_{Na}(t, V) = g_{Na}^{max} (1 + e\delta_{Na} \sigma_3(W_{Na})) \mathcal{M}_{Na}^p(t, V) \mathcal{H}_{Na}^q(t, V)$$

We can also handle the the case of the Ca^{++} and neurotransmitter triggers. These details can be found in (Peterson

(5) 2005) and so will not be given here. We simply note that in these cases $[T_0]$ represents $[Ca^{++}]$ and $[T_1]$ will denote some sort of Ca^{++} binding complex. To see how a neurotransmitter modulator can be handled, we consider the general model shown in Figure 5(a). The dendrite is modeled as a Rall cable of electrotonic length L_1 and the soma is a cylinder of length L_2 . Both the Rall cable and the soma can receive excitatory and / or inhibitory current pulses generally denoted by the letters ESP and ISP. When the output of one neuron is sent into the input system of another, we typically call the neuron providing the input the *pre-neuron* and the neuron generating the output, the *post-neuron*. The axon of the pre-neuron interacts with the dendrite of the post-neuron via a structure called the *post synaptic density* or *PSD*. The pre-neuron generates an axonal pulse which is the input to the PSD structure. The PSD is really a computational object which transduces the axonal voltage signal on the pre-axon into a ESP or ISP on the post-dendrite cable. The pre-neuron's action potential influences the release of the contents of synaptic vesicles into the fluid contained in the region between the neurons. Remember, the brain is a 3D organ and all neurons are enclosed by a liquid soup of water and many other chemicals. The vesicles contain *neurotransmitters*. For convenience, we focus on one such neurotransmitter, labeled ζ . The vesicle containing ζ is inside a structure called a spine on the surface of the pre-axon. The vesicle migrates to the wall of the spine and then through the wall itself so that it is exposed to the fluid between the pre-axon and post-dendrite (the synaptic cleft). The vesicle ruptures and spreads the ζ neurotransmitter into the synaptic cleft. The ζ neurotransmitter then acts like the trigger T_0 we have already discussed. It binds in some fashion to a port or gate specialized for the λ neurotransmitter. The neurotransmitter ζ then initiates a cascade of reactions:

- It passes through the gate, entering the interior of the cable. It then forms a complex, $\hat{\zeta}$.
- Inside the post-dendrite, $\hat{\zeta}$ influences the passage of ions through the cable wall. For example, it may increase the passage of Na^+ through the membrane of the cable thereby initiating an ESP. It could also influence the formation of a calcium current, an increase in K^+ and so forth.
- The influence via $\hat{\zeta}$ can be that of a second messenger trigger.

Hence, each neuron creates a brew of neurotransmitters specific to its type. A trigger of type T_0 can thus influence the production of neurotransmitters with concomitant changes in post-neuron activity. Thus, in addition to modeling Ca^{++} or other triggers as mechanisms to alter the maximum sodium and potassium conductance, we can also model triggers that provide ways to increase or decrease neurotransmitter. Since the neurotransmitter ζ is a second messenger trigger, we obtain, leaving off most of the earlier steps in the computation, the usual output equation

$$h^\zeta([P^\zeta([\hat{\zeta}](t)]) = \frac{e^\zeta}{2} \delta_\zeta g_\zeta^{max} \left(1 + \tanh\left(\frac{[P^\zeta(\hat{\zeta}(t))]}{g^\zeta}\right) \right)$$

The final step is to interpret what function the protein P^λ has in the cellular system. If it is a sodium or potassium gate, the modification of the conductance of those ions is as before:

$$g_a(t, V) = (g_a^{max} + h([P([\hat{\zeta}](t))])\mathcal{M}_a^p(t, V)\mathcal{H}_a^q(t, V)$$

However, the protein could increase calcium current by adding more calcium gates. We can model the calcium current alterations as

$$Ca^{++}(t, V) = (Ca^{++})_\zeta^{max} + h_\zeta([P([\hat{\zeta}](t))])$$

This gives the sodium and potassium influence equations

$$\delta g_\lambda^{max}(t, x) = \sum_{\zeta_s} \frac{h_\zeta([P^\zeta([\hat{\zeta}](t))])}{t - t_{\zeta_s}} \exp\left(\frac{-(x - x_{\zeta_s})^2}{4D_{\zeta_s}(t - t_{\zeta_s})}\right)$$

where the index ζ_s denotes the sites where the ζ gates are located. If the neurotransmitter modifies the calcium currents, we have a different type of influence:

$$\delta(Ca^{++})_\zeta^{max}(t, x) = \sum_{\zeta_s} h_\zeta([P^\zeta([\hat{\zeta}](t))])$$

We will be focusing on only a few neurotransmitters. We will use ζ_0 as the designation for the neurotransmitter *serotonin*; ζ_1 , for *dopamine* and ζ_2 , for *norepinephrine*. In Figure 5(a), we show a typical computational neuron assembly. The dendritic cable is electronic distance L_1 and we will use the variable w to denote distance along the dendrite. The soma is also modeled as a cylinder and we assume it can receive input at electronic distances up to L_2 away from the axon hillock. The inputs to the dendrite occur through ports P_D and the soma entry ports are labeled by P_S . We have a variety of inputs that enter the dendrite. For each time t_0 , we sum over the dendrite distance, the effects of all the inputs. These include

- a trigger T_0 which enters the dendrite port P_D and is a simple modulator of the voltage activated gates for sodium and potassium. So we directly modify the maximum ion conductance.
- a trigger T_0 which is a second messenger whose effects on sodium and ion conductance utilize a sigmoid - 3 transition.

- a Ca^{++} injection current which can alter the sodium and potassium conductance functions via second messenger pathways.
- neurotransmitters λ_0 to λ_4 which can modify sodium and potassium conductance via second messenger effects or directly. In addition, they can alter calcium currents via second messenger pathways.

5 The Abstract Neuron Model

The general structure of a typical action potential is illustrated in Figure 5(b). This wave form is idealized and we are interested in how much information can be transferred from one abstract neuron to another using a low dimensional biologically based feature vector (BFV). We can achieve such an abstraction by noting that in a typical excitable neuron response, Figure 5(b), the action potential exhibits a combination of cap-like shapes.

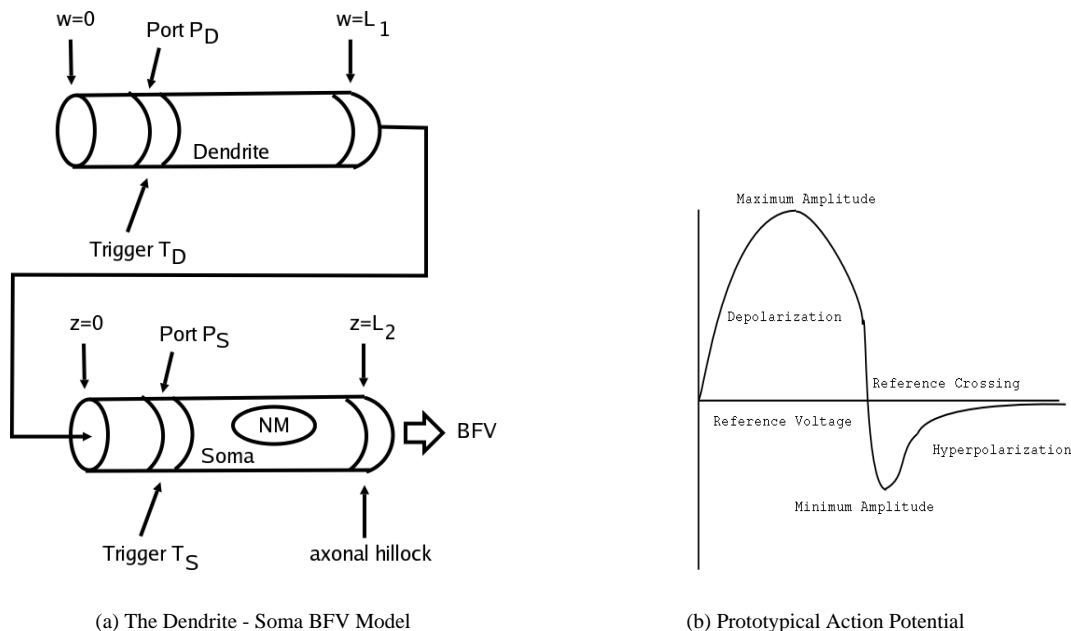


Figure 5: Neuron Computation

We can use the following points on this generic action potential to construct a low dimensional feature vector of Equation 17. Note that $V'_m(t_3) = (V_4 - V_3) g$.

$$\xi = \left\{ \begin{array}{ll} (t_0, V_0) & \text{start point} \\ (t_1, V_1) & \text{maximum point} \\ (t_2, V_2) & \text{return to reference voltage} \\ (t_3, V_3) & \text{minimum point} \\ (g, t_4, V_4) & \text{sigmoid model of tail} \\ & V_3 + (V_4 - V_3) \tanh(g(t - t_3)) \end{array} \right\} \quad (17)$$

where the model of the tail of the action potential is of the form $V_m(t) = V_3 + (V_4 - V_3) \tanh(g(t - t_3))$. Note that $V'_m(t_3) = (V_4 - V_3) g$ and so if we were using real voltage data, we could approximate $V'_m(t_3)$ by a standard finite difference. The feature vector stores many of the important features of the action potential in a low dimensional form. We note these include

- The interval $[t_0, t_1]$ is the duration of the rise phase. This interval can be altered or modulated by neurotransmitter activity on the nerve cell's membrane as well as second messenger signaling from within the cell.
- The height of the pulse, V_1 , is an important indicator of excitation.
- The time interval between the highest activation level, V_1 and the lowest, V_3 , is closely related to spiking interval. This time interval, $[t_1, t_3]$, is also amenable to alteration via neurotransmitter input.
- The “height” of the depolarizing pulse, V_4 , helps determine how long it takes for the neuron to reestablish its reference voltage, V_0 .
- The neuron voltage takes time to reach reference voltage after a spike. This is the time interval by the interval $[t_3, \infty]$.
- The exponential rate of increase in the time interval $[t_3, \infty]$ is also very important to the regaining of nominal neuron electrophysiological characteristics.

Clearly, we can model an inhibitory pulse in essentially the same way, *mutatis mutandi*. We will assume all of the data points in our feature vector are potentially mutable due to neurotransmitter activity, input pulses into the neuron's dendritic system and alteration of the neuron hardware via genome access with the second messenger system. We believe the simple biological feature vector (BFV) can be used to discriminate subtle changes in the action potential wave form as is detailed in (Peterson and Khan (7) 2005-1) . Hence, one could use ensembles of abstract neurons whose outputs are BFVs (11 dimensional say) to create local cortical computationally phase locked groups. The effects of modulatory agents such as neurotransmitters can be modeled as introducing changes in the BFVs. The kinds of changes one should use for a given neurotransmitters modulatory effect can be estimated from the biophysical and

toxin literature. An increase in sodium ion flow, Ca⁺² gated second messenger activity can be handled at a high level as a suitable change in one of the 11 parameters of the BFV.

5.1 The BFV Functional Form:

In Figure 6(a), we indicated the three major portions of the biological feature vector and the particular data points chosen from the action potential which are used for the model. These are the two parabolas f_1 and f_2 and the sigmoid f_3 . The parabola f_1 is treated as the two distinct pieces f_{11} and f_{12} given by

$$f_{11}(t) = a^{11} + b^{11}(t - t_1)^2 \quad (18)$$

$$f_{12}(t) = a^{12} + b^{12}(t - t_1)^2 \quad (19)$$

$$(20)$$

Thus, f_1 consists of two joined parabolas which both have a vertex at t_1 . The functional form for f_2 is a parabola with vertex at t_3 :

$$f_2(t) = a^2 + b^2(t - t_3)^2 \quad (21)$$

$$(22)$$

Finally, the sigmoid portion of the model is given by

$$f_3(t) = V_3 + (V_4 - V_3) \tanh(g(t - t_3)) \quad (23)$$

We have also simplified the BFV even further by dropping the explicit time point t_4 and modeling the portion of the action potential after the minimum voltage by the sigmoid f_3 .

From the data, it follows that

$$f_{11}(t_0) = V_0 = a^{11} + b^{11}(t_0 - t_1)^2$$

$$f_{11}(t_1) = V_1 = a^{11}$$

$$f_{12}(t_1) = V_1 = a^{12}$$

$$f_{11}(t_2) = V_2 = a^{12} + b^{12}(t_2 - t_1)^2$$

This implies

$$\begin{aligned} a^{11} &= V_1 \\ b^{11} &= \frac{V_0 - V_1}{(t_0 - t_1)^2} \\ a^{12} &= V_1 \\ b^{12} &= \frac{V_2 - V_1}{(t_2 - t_1)^2} \end{aligned}$$

In a similar fashion, the f_2 model is constrained by

$$\begin{aligned} f_2(t_2) &= V_2 = a^2 + b^2(t_2 - t_3)^2 \\ f_2(t_3) &= V_3 = a^2 \end{aligned}$$

We conclude that

$$\begin{aligned} a^2 &= V_3 \\ b^2 &= \frac{V_2 - V_3}{(t_2 - t_3)^2} \end{aligned}$$

Hence, the functional form of the BFV model can be given by the mapping f of equation 24.

$$f(t) = \begin{cases} V_1 + \frac{V_0 - V_1}{(t_0 - t_1)^2}(t - t_1)^2, & t_0 \leq t \leq t_1 \\ V_1 + \frac{V_2 - V_1}{(t_2 - t_1)^2}(t - t_1)^2, & t_1 \leq t \leq t_2 \\ V_3 + \frac{V_2 - V_3}{(t_2 - t_3)^2}(t - t_3)^2, & t_2 \leq t \leq t_3 \\ V_4 + (V_4 - V_3) \tanh(g(t - t_3)), & t_3 \leq t < \infty \end{cases} \quad (24)$$

All of our parabolic models can also be written in the form

$$p(t) = \pm \frac{1}{4\beta}(t - \alpha)$$

where 4β is the width of the line segment through the focus of the parabola. The models f_{11} and f_{12} point down and so use the “minus” sign while f_2 uses the “plus”. By comparing our model equations with this generic parabolic equation, we find the width of the parabolas of f_{11} , f_{12} and f_2 is given by

$$\begin{aligned} 4\beta_{11} &= \frac{(t_0 - t_1)^2}{V_1 - V_0} = \frac{-1}{b^{11}} \\ 4\beta_{12} &= \frac{(t_2 - t_1)^2}{V_1 - V_2} = \frac{-1}{b^{12}} \\ 4\beta_2 &= \frac{(t_2 - t_3)^2}{V_2 - V_3} = \frac{1}{b^2} \end{aligned}$$

5.2 Modulation of the BFV Curve:

We want to modulate the output of our abstract neuron model by altering the BFV. The BFV itself consists of 10 parameters, but better insight, into how alterations of the BFV introduce changes in the “action potential” we are creating, comes from studying changes in the mapping f given in Section 5.1. In addition to changes in timing, t_0 , t_1 , t_2 and t_3 , we can also consider the variations of Equation 25.

$$\begin{bmatrix} \Delta a^{11} \\ \Delta b^{11} \\ \Delta a^{12} \\ \Delta b^{12} \\ \Delta a^2 \\ \Delta b^2 \end{bmatrix} = \begin{bmatrix} \Delta V_1 \\ \Delta\left(\frac{V_0 - V_1}{(t_0 - t_1)^2}\right) \\ \Delta V_1 \\ \Delta\left(\frac{V_2 - V_1}{(t_2 - t_1)^2}\right) \\ \Delta V_3 \\ \Delta\left(\frac{V_2 - V_3}{(t_2 - t_3)^2}\right) \end{bmatrix} = \begin{bmatrix} \Delta \text{Maximum Voltage} \\ \Delta\left(\frac{-1}{4\beta_{11}}\right) \\ \Delta \text{Maximum Voltage} \\ \Delta\left(\frac{-1}{4\beta_{12}}\right) \\ \Delta \text{Minimum Voltage} \\ \Delta\left(\frac{1}{4\beta_2}\right) \end{bmatrix} \quad (25)$$

It is clear that modulatory inputs that alter the cap shape and hyperpolarization curve of the BFV functional form can have a profound effect on the information contained in the “action potential”. For example, a hypothetical neurotransmitter that alters V_1 will also alter the latis rectum distance across the cap f_1 . Further, direct modifications to the latis rectum distance in any of the two caps f_{11} and f_{12} can induce corresponding changes in times t_0 , t_1 and t_2 and voltages V_0 , V_1 and V_2 . A similar statement can be made for changes in the latis rectum of cap f_2 . For example, if a neurotransmitter induced a change of, say 1% in $4\beta_{11}$, this would imply that $\Delta\left(\frac{V_1 - V_0}{(t_0 - t_1)^2}\right) = .04\beta_{11}^0$ where β_{11}^0 denotes the original value of β_{11}^0 . Thus, to first order

$$.04\beta_{11}^0 = \left(\frac{\partial\beta_{11}}{\partial V_0}\right)^* \Delta V_0 + \left(\frac{\partial\beta_{11}}{\partial V_1}\right)^* \Delta V_1 + \left(\frac{\partial\beta_{11}}{\partial t_0}\right)^* \Delta t_0 + \left(\frac{\partial\beta_{11}}{\partial t_1}\right)^* \Delta t_1 \quad (26)$$

where the superscript * on the partials indicates they are evaluated at the base point (V_0, V_1, t_0, t_1) . Taking partials we

find

$$\begin{aligned} \left(\frac{\partial \beta_{11}}{\partial V_0}\right) &= 2 \frac{(t_0 - t_1)^2}{(V_1 - V_0)^2} = \frac{2}{V_1 - V_0} \beta_{11}^0 \\ \left(\frac{\partial \beta_{11}}{\partial V_1}\right) &= -2 \frac{(t_0 - t_1)^2}{(V_1 - V_0)^2} = -\frac{2}{V_1 - V_0} \beta_{11}^0 \\ \left(\frac{\partial \beta_{11}}{\partial t_0}\right) &= 2 \frac{t_0 - t_1}{V_1 - V_0} = \frac{2}{t_0 - t_1} \beta_{11}^0 \\ \left(\frac{\partial \beta_{11}}{\partial t_1}\right) &= -2 \frac{t_0 - t_1}{V_1 - V_0} = -\frac{2}{t_0 - t_1} \beta_{11}^0 \end{aligned}$$

Thus, Equation 26 becomes

$$.04 \beta_{11}^0 = \frac{2 \Delta V_0}{V_1 - V_0} \beta_{11}^0 - \frac{2 \Delta V_1}{V_1 - V_0} \beta_{11}^0 + 2 \Delta t_0 \frac{1}{t_0 - t_1} \beta_{11}^0 - 2 \Delta t_1 \frac{1}{t_0 - t_1} \beta_{11}^0$$

This simplifies to

$$.02(V_1 - V_0)(t_0 - t_1) = (\Delta V_0 - \Delta V_1)(t_0 - t_1) - (\Delta t_0 - \Delta t_1)(V_1 - V_0)$$

Since we can do this analysis for any percentage r of β_{11}^0 , we can infer that a neurotransmitter that modulates the action potential by perturbing the “width” or latis rectum of the cap of f_{11} can do so satisfying the equation

$$2r(V_1 - V_0)(t_1 - t_0) = (\Delta V_0 - \Delta V_1)(t_0 - t_1) - (\Delta t_0 - \Delta t_1)(V_1 - V_0)$$

Similar equations can be derived for the other two width parameters for caps f_{12} and f_3 . These sorts of equations give us design principles for complex neurotransmitter modulations of a BFV.

5.3 The BFV Ball and Stick Neuron:

The BFV model we build consists of a dendritic system and a computational core which processed BFV input sequence to generate a BFV output.

Consider a typical input $V(t)$ which is determined by a BFV vector. Without loss of generality, we will focus on excitatory inputs in our discussions. The input consists of a three distinct portions. First, a parabolic cap above the equilibrium potential determined by the values (t_0, V_0) , (t_1, V_1) , (t_2, V_2) . Next, the input contains half of another

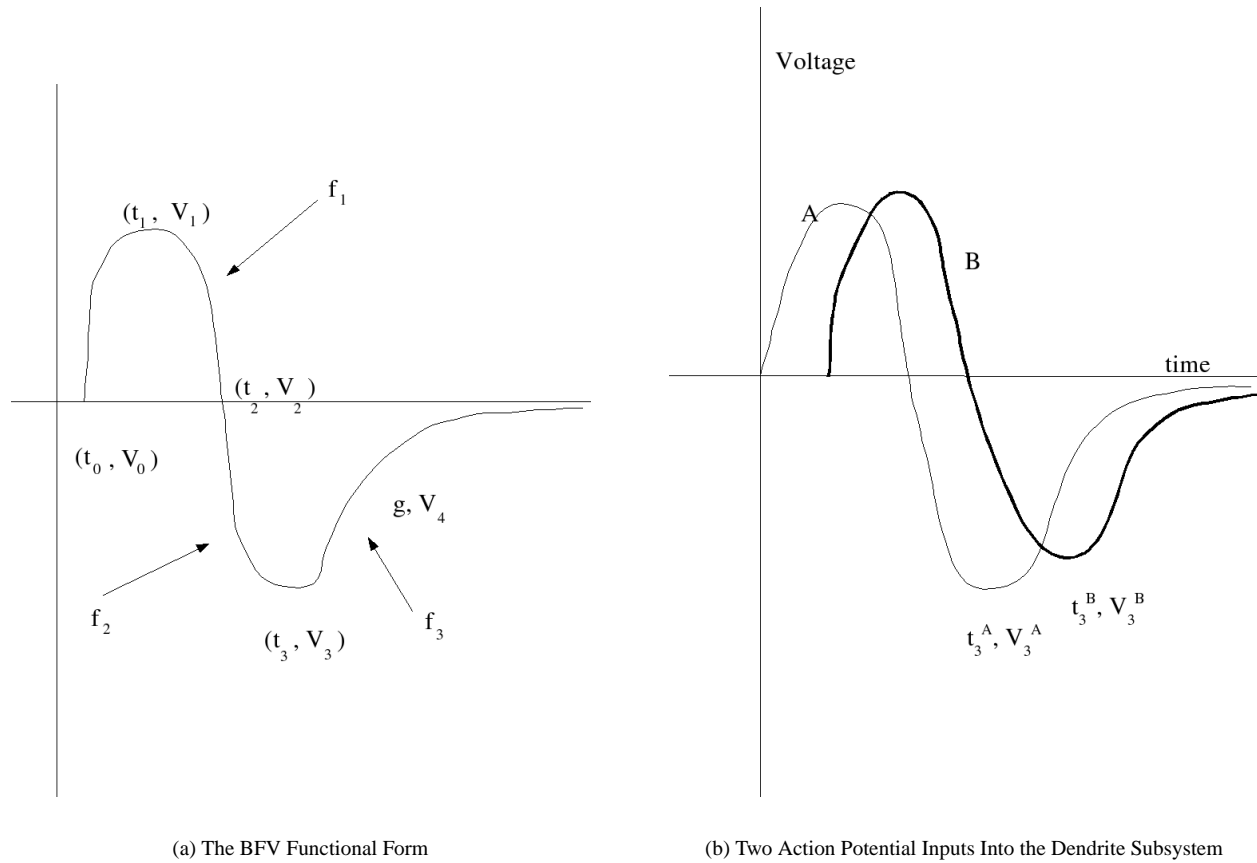


Figure 6: BFV Inputs

parabolic cap dropping below the equilibrium potential determined by the values (t_2, V_2) and (t_3, V_3) . Finally, there is the hyperpolarization phase having functional form $H(t) = V_3 + (V_4 - V_3) \tanh(g(t - t_3))$. Now assume two inputs arrive at the same electronic distance L . We label this inputs as A and B as is shown in Figure 6(b). For convenience of exposition, we also assume $t_3^A < t_3^B$, as otherwise, we just reverse the roles of the variables in our arguments. In this figure, we note only the minimum points on the A and B curves. We merge these inputs into a new input V^N prior to the hyperpolarization phase as follows:

$$\begin{aligned}
 t_0^N &= \frac{t_0^A + t_0^B}{2} \\
 V_0^N &= \frac{V_0^A + V_0^B}{2} \\
 t_1^N &= \frac{t_1^A + t_1^B}{2} \\
 V_1^N &= \frac{V_1^A + V_1^B}{2} \\
 t_2^N &= \frac{t_2^A + t_2^B}{2} \\
 V_2^N &= \frac{V_2^A + V_2^B}{2}
 \end{aligned}$$

This constructs the two parabolic caps of the new resultant input by averaging the caps of V^A and V^B . The construction of the new hyperpolarization phase is more complicated. The shape of this portion of an action potential has a profound effect on neural modulation, so it is very important to merge the two inputs in a reasonable way. The hyperpolarization phases of V^A and V^B are given by

$$\begin{aligned} H^A(t) &= V_3^A + (V_4^A - V_3^A) \tanh(g^A(t - t_3^A)) \\ H^B(t) &= V_3^B + (V_4^B - V_3^B) \tanh(g^B(t - t_3^B)) \end{aligned}$$

We will choose the 4 parameters V_3, V_4, g, t_3 so as to minimize

$$E = \int_{t_3^A}^{\infty} (H(t) - H^A(t))^2 + (H(t) - H^B(t))^2 dt$$

For optimality, we find the parameters where $\frac{\partial E}{\partial V_3}, \frac{\partial E}{\partial V_4}, \frac{\partial E}{\partial g}$ and $\frac{\partial E}{\partial t_3}$ are 0. Now,

$$\frac{\partial E}{\partial V_3} = \int_{t_3^A}^{\infty} 2\{(H(t) - H^A(t)) + (H(t) - H^B(t))\} \frac{\partial H}{\partial V_3} dt$$

Further,

$$\frac{\partial H}{\partial V_3} = 1 - \tanh(g(t - t_3))$$

so we obtain

$$0 = \int_{t_3^A}^{\infty} 2\{(H(t) - H^A(t)) + (H(t) - H^B(t))\} (1 - \tanh(g(t - t_3))) dt \quad (27)$$

We also find

$$\frac{\partial E}{\partial V_4} = \int_{t_3^A}^{\infty} 2\{(H(t) - H^A(t)) + (H(t) - H^B(t))\} (\tanh(g(t - t_3))) dt$$

as

$$\frac{\partial H}{\partial V_4} = \tanh(g(t - t_3))$$

The optimality condition then gives

$$0 = \int_{t_3^A}^{\infty} 2\{(H(t) - H^A(t)) + (H(t) - H^B(t))\} \tanh(g(t - t_3)) dt \quad (28)$$

Combining equation 27 and equation 28, we find

$$\begin{aligned} 0 &= \int_{t_3^A}^{\infty} \{(H(t) - H^A(t)) + (H(t) - H^B(t))\} dt \\ &\quad - \int_{t_3^A}^{\infty} \{(H(t) - H^A(t)) + (H(t) - H^B(t))\} \tanh(g(t - t_3)) dt \\ 0 &= \int_{t_3^A}^{\infty} \{(H(t) - H^A(t)) + (H(t) - H^B(t))\} \tanh(g(t - t_3)) dt. \end{aligned}$$

It follows after simplification, that

$$0 = \int_{t_3^A}^{\infty} \{(H(t) - H^A(t)) + (H(t) - H^B(t))\} dt \quad (29)$$

The remaining optimality conditions give

$$\begin{aligned} \frac{\partial E}{\partial g} &= \int_{t_3^A}^{\infty} 2\{(H(t) - H^A(t)) + (H(t) - H^B(t))\} \frac{\partial H}{\partial g} dt = 0 \\ \frac{\partial E}{\partial t_3} &= \int_{t_3^A}^{\infty} 2\{(H(t) - H^A(t)) + (H(t) - H^B(t))\} \frac{\partial H}{\partial t_3} dt = 0 \end{aligned}$$

We calculate

$$\begin{aligned} \frac{\partial H}{\partial g} &= (V_4 - V_3)(t - t_3) \operatorname{sech}^2(g(t - t_3)) \\ \frac{\partial H}{\partial t_3} &= -(V_4 - V_3)g \operatorname{sech}^2(g(t - t_3)) \end{aligned}$$

Thus, we find

$$0 = \int_{t_3^A}^{\infty} \{(H(t) - H^A(t)) + (H(t) - H^B(t))\} (V_4 - V_3)(t - t_3) \operatorname{sech}^2(g(t - t_3)) dt$$

$$0 = \int_{t_3^A}^{\infty} \{(H(t) - H^A(t)) + (H(t) - H^B(t))\} (V_4 - V_3) g \operatorname{sech}^2(g(t - t_3)) dt.$$

This implies

$$0 = \int_{t_3^A}^{\infty} \{(H(t) - H^A(t)) + (H(t) - H^B(t))\} t \operatorname{sech}^2(g(t - t_3)) dt$$

$$- t_3 \int_{t_3^A}^{\infty} \{(H(t) - H^A(t)) + (H(t) - H^B(t))\} \operatorname{sech}^2(g(t - t_3)) dt$$

$$0 = \int_{t_3^A}^{\infty} \{(H(t) - H^A(t)) + (H(t) - H^B(t))\} \operatorname{sech}^2(g(t - t_3)) dt.$$

This clearly can be simplified to

$$0 = \int_{t_3^A}^{\infty} \{(H(t) - H^A(t)) + (H(t) - H^B(t))\} t \operatorname{sech}^2(g(t - t_3)) dt$$

We can satisfy equation 29 and equation 30 by making

$$(H(t) - H^A(t)) + (H(t) - H^B(t)) = 0. \quad (30)$$

Equation 30 can be rewritten as

$$0 = (V_3 - \frac{V_3^A + V_3^B}{2}) + (V_4 - V_3) \tanh(g(t - t_3)) \quad (31)$$

$$- \frac{V_4^B - V_3^B}{2} \tanh(g^B(t - t_3^B)) - \frac{V_4^A - V_3^A}{2} \tanh(g^A(t - t_3^A)) \quad (32)$$

This equation is true as $t \rightarrow \infty$. Thus, we obtain the identity

$$0 = (V_3 - \frac{V_3^A + V_3^B}{2}) + (V_4 - V_3) - \frac{V_4^B - V_3^B}{2} - \frac{V_4^A - V_3^A}{2}$$

Upon simplification, we find

$$0 = \left(V_3 - \frac{V_3^A + V_3^B}{2}\right)$$

$$0 = \left(V_4 - \frac{V_4^A + V_4^B}{2}\right)$$

This leads to our choices for V_3 and V_4 .

$$V_3 = \frac{V_3^A + V_3^B}{2} \quad (33)$$

$$V_4 = \frac{V_4^A + V_4^B}{2} \quad (34)$$

Equation 32 is also true at $t = t_3^A$ and $t = t_3^B$. This gives

$$0 = \left(V_3 - \frac{V_3^A + V_3^B}{2}\right) + (V_4 - V_3) \tanh(g(t_3^A - t_3)) - \frac{V_4^B - V_3^B}{2} \tanh(g^B(t_3^A - t_3^B)) \quad (35)$$

$$0 = \left(V_3 - \frac{V_3^A + V_3^B}{2}\right) + (V_4 - V_3) \tanh(g(t_3^B - t_3)) - \frac{V_4^A - V_3^A}{2} \tanh(g^A(t_3^B - t_3^A)) \quad (36)$$

$$(37)$$

For convenience, define $w_{34}^A = \frac{V_4^A - V_3^A}{2}$ and $w_{34}^B = \frac{V_4^B - V_3^B}{2}$. Then, using equation 34, equation 36 and equation 37 become

$$0 = (V_4 - V_3) \tanh(g(t_3^A - t_3)) - w_{34}^B \tanh(g^B(t_3^A - t_3^B))$$

$$0 = (V_4 - V_3) \tanh(g(t_3^B - t_3)) - w_{34}^A \tanh(g^A(t_3^B - t_3^A))$$

This is then rewritten as

$$\tanh(g(t_3^A - t_3)) = \frac{w_{34}^B \tanh(g^B(t_3^A - t_3^B))}{(V_4 - V_3)}$$

$$\tanh(g(t_3^B - t_3)) = \frac{w_{34}^A \tanh(g^A(t_3^B - t_3^A))}{(V_4 - V_3)}$$

Defining

$$z_A = \frac{w_{34}^B \tanh(g^B(t_3^A - t_3^B))}{V_4 - V_3}$$

$$z_B = \frac{w_{34}^A \tanh(g^A(t_3^B - t_3^A))}{V_4 - V_3}$$

we find that the optimality conditions have led to the two nonlinear equations for g and t_3 given by

$$\tanh(g(t_3^A - t_3)) = z_A \quad (38)$$

$$\tanh(g(t_3^B - t_3)) = z_B \quad (39)$$

Note that using equation 34 and equation 34, we have

$$z_A = \frac{w_{34}^B \tanh(g^B(t_3^A - t_3^B))}{V_4 - V_3}$$

$$= \frac{w_{34}^B \tanh(g^B(t_3^B - t_3^A))}{w_{34}^A + w_{34}^B}$$

$$z_B = \frac{w_{34}^A \tanh(g^A(t_3^B - t_3^A))}{V_4 - V_3}$$

$$= \frac{w_{34}^A \tanh(g^A(t_3^B - t_3^A))}{w_{34}^A + w_{34}^B}$$

Hence,

$$z_A > -\frac{w_{34}^B}{w_{34}^A + w_{34}^B} > -1$$

$$z_B < \frac{w_{34}^A}{w_{34}^A + w_{34}^B} < 1$$

so that $z_A < 0 < z_B$. It seems reasonable that the optimal value of t_3 should lie between t_3^A and t_3^B . Note equation 39 and equation 39 preclude the solutions $t_3 = t_3^A$ or $t_3 = t_3^B$. To solve the nonlinear system for g and t_3 , we will approximate \tanh by its first order Taylor Series expansion. This seems reasonable as we don't expect $g(t_3^A - t_3)$ and $g(t_3^B - t_3)$ to be far from 0. This gives the approximate system

$$g(t_3^A - t_3) \approx z_A \quad (40)$$

$$g(t_3^B - t_3) \approx z_B \quad (41)$$

From equation 41, we find

$$g = \frac{z_B}{t_3^B - t_3}$$

Substituting this into equation 41, we obtain

$$\frac{z_B}{t_3^B - t_3} (t_3^A - t_3) = z_A$$

This can be simplified as follows:

$$\begin{aligned} \frac{t_3^A - t_3}{t_3^B - t_3} &= \frac{z_A}{z_B} \\ (t_3^A - t_3)z_B &= (t_3^B - t_3)z_A \\ t_3^A z_B - t_3^B z_A &= t_3(z_B - z_A) \end{aligned}$$

Thus, we find the optimal value of t_3 is approximately

$$t_3 = \frac{t_3^A z_B - t_3^B z_A}{z_B - z_A} \quad (42)$$

Using the approximate value of t_3 , we find the optimal value of g can be approximated as follows:

$$\begin{aligned} g &= \frac{z_B}{t_3^B - \frac{t_3^A z_B - t_3^B z_A}{z_B - z_A}} \\ &= \frac{z_B(z_B - z_A)}{t_3^B(z_B - z_A) - (t_3^A z_B - t_3^B z_A)} \\ &= \frac{z_B(z_B - z_A)}{t_3^B z_B - t_3^A z_B} \\ &= \frac{z_B - z_A}{t_3^B - t_3^A} \end{aligned}$$

Hence, we find the approximate optimal value of g is

$$g = \frac{z_B - z_A}{t_3^B - t_3^A} \quad (43)$$

It is easy to check that this value of t_3 lies in (t_3^A, t_3^B) as we suspected it should and that g is positive. We summarize our results. Given two input BFVs, the sigmoid portions of the incoming BFVs combine into the new sigmoid given by

$$\begin{aligned} H(t) &= V_3 + (V_4 - V_3) \tanh(g(t - t_3)) \\ H(t) &= \frac{V_3^A + V_3^B}{2} + \left(\frac{V_4^A - V_3^A}{2} + \frac{V_4^B - V_3^B}{2} \right) \tanh\left(\frac{z_B - z_A}{t_3^B - t_3^A} \left(t - \frac{t_3^A z_B - t_3^B z_A}{z_B - z_A}\right)\right) \end{aligned}$$

Given an input sequence of BFV's into a port on the dendrite of an accepting neuron

$$\{V_n, V_{n-1}, \dots, V_1\}$$

the procedure discussed above computes the combined response that enters that port at a particular time. The inputs into the dendritic system are combined pairwise; V_2 and V_1 combine into a V_{new} which then combines with V_3 and so on. We can do this at each electrotonic location. Since more than one pre-neuron axon can provide input to a given electrotonic location on the dendrite cable of our model, the algorithm above provides the mechanism we need to combine multiple incoming BFVs into one merged BFV.

5.4 The Full Abstract Neuron Model:

A neuron accepts inputs from its innervating collection of pre-neuron axonal outputs. Such pre-neurons supply input to the dendrite cable at electronic positions $w = 0$ to $w = 4$. These inputs generate an ESP or ISP via many possible mechanisms or they alter the structure of the dendrite cable itself by the transcription of proteins. The output of a pre-neuron is a BFV which must then be associated with an abstract trigger as we have discussed earlier. The strength of a BFV output will be estimated as follows: The area under the first parabolic cap of the BFV can be approximated by the area of the triangle, A , formed by the vertices (t_0, V_0) , (t_1, V_1) , (t_2, V_2) . The area is given by $A = \frac{1}{2}(V_2 - V_0)(t_2 - t_0)$. The pre-neuron signals that come into the dendritic cable of the post-neuron are the initial conditions that determined the voltage at the axon hillock of the post-neuron. We are modeling the dendritic arbor and the soma as finite length cables. At position λ on the cable, the voltage is given by

$$\hat{v}_m(\lambda, \tau) = A_0 e^{-\tau} + \sum_{n=1}^{\infty} A_n \cos(\alpha_n(4 - \lambda)) e^{-(1+\alpha_n^2)\tau}$$

as discussed in Section 2.1. This voltage arrives at the far end, $z = 7$ in Figure 7, of the soma cable and the voltage we have at $z = 0$ is then the axon hillock voltage. This figure shows a general computational architecture for an artificial neuron consisting of

- a dendrite system of electronic length 4. Four dendrite ports are shown labeled as D_i . Each accepts ISP and ESP inputs which are generated and modulated using the mechanisms we have discussed.
- a soma of length 7 which contains 7 pairs simple and second messenger ports (G_i and SM_i , respectively). The simple ports G_i are where sodium and potassium maximum conductance can be modified by direct means. The second messenger ports SM_i accept trigger T_0 and generate proteins which alter the functionality of the cell by accessing the genome.
- Three nuclear membrane gate blocks, NG_i where second messenger proteins T_1 can dock to initiate the transcription of a protein used in altering cell function.
- The protein block is shown differentiating into the gate proteins that are sent to the sites G_i . Although not shown, there could also be proteins that alter Ca^{++} injection currents

The axon hillock voltage is then input into the Hodgkin - Huxley equations to generate an action potential. The voltage at $z = 0$ would have the form

$$\hat{v}_m(0, \tau) = B_0 e^{-\tau} + \sum_{n=1}^{\infty} B_n \cos(7\beta_n) e^{-(1+\beta_n^2)\tau}$$

Efficient ways to compute the axon hillock voltage are discussed in (Peterson (5) 2005) . In general, the discussions above shows us how to define classes of neurons that all have a similar structure. The neuron class \mathcal{O} axon hillock voltage computation will explicitly depend on certain structural characteristics of the input system:

- L , the length of the cable,
- L_e , the electrotonic length,
- The value of $\rho = \frac{G_D}{G_S}$, the ratio of the dendritic conductance to soma conductance,
- The solution to the eigenvalue equation

$$\tan(\alpha L) = -\frac{\tanh(L)}{\rho L}(\alpha L),$$

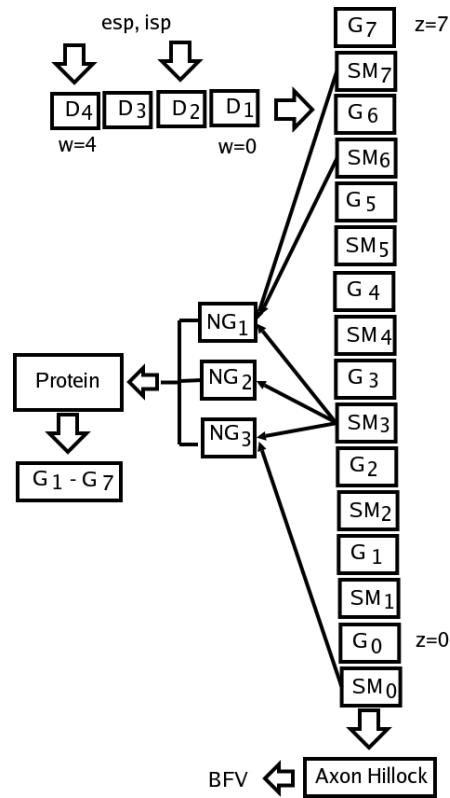


Figure 7: Cellular Agent Computations

- N , the number of eigenfunctions to use in our expansions,

Thus, we can define a neuron class for each possible choice of this parameter set. It is clear neuron classes can have different trigger characteristics. First, consider the case of neurons which create the monoamine neurotransmitters. Neurons of this type in the Reticular Formation of the midbrain produce a monoamine neurotransmitter packet at the synaptic junction between the axon of the pre-neuron and the dendrite of the post-neuron. The monoamine neurotransmitter is then released into the synaptic cleft and it induces a second messenger response. The strength of this response is dependent on the BFV input from pre-neurons that form synaptic connections with the post-neuron. We compute the BFV coming in via the algorithm for combining different BFV's discussed in Section 5.3. The strength of this input determines the strength of the monoamine trigger into the post-neuron dendrite. Let the strength be given by the weighting term $c_{pre,post}^\zeta$ where as usual we use the values $\zeta = 0$ to denote the neurotransmitter serotonin, $\zeta = 1$, for dopamine and $\zeta = 2$, for norepinephrine. In our model, recall that time is discretized into integer values as time ticks 1, 2 and so forth via our global simulation clock. Also, spatial values are discretized into multiples of various electrotonic scaling distances. With that said, the trigger at time t and dendrite location w is therefore

$$T_0(t, w) = \frac{c_{pre,post}^\zeta}{\sqrt{t - t_0}} \exp\left(\frac{-(w - w_0)^2}{4D_0^\zeta(t - t_0)}\right).$$

where D_0^ζ is the diffusion constant associated with the trigger. Hence, $w = j\hat{L}_E$ for some scaling \hat{L}_E . The trigger T_0 has associated with it the protein T_1 . We let

$$T_1(t, w) = \frac{d_{pre,post}^\zeta}{\sqrt{t-t_0}} \exp\left(\frac{-(w-w_0)^2}{4D_1^\zeta(t-t_0)}\right).$$

where $d_{pre,post}^\zeta$ denotes the strength of the induced T_1 response and D_1^ζ is the diffusion constant of the T_1 protein. This trigger will act through the usual pathway. Also, we let T_2 denote the protein $P(T_1)$. T_2 transcribes a protein target from the genome with efficiency e .

$$[T_2](t, w) = h_{T_2}(t, w)[T_2]_n$$

Note $[T_2](t, w)$ gives the value of the protein T_2 concentration at some discrete time t and spatial location $j\hat{L}_E$. This response can also be modulated by feedback. In this case, let ξ denote the feedback level. Then, the final response is altered to $h_{T_2}^f$ where the superscript f denotes the feedback response and the constant ω is the strength of the feedback.

$$\begin{aligned} h_{T_2}^f(t, w) &= \omega \frac{1}{\xi} h_{T_2}(t, w) \\ [T_2](t, w) &= h_{T_2}^f(t, w)[T_2]_n \end{aligned}$$

There are a large number of shaping parameters here. For example, for each neurotransmitter, we could alter the parameters due to calcium trigger diffusion. These would include D_0^ζ , the diffusion constant for the trigger, and D_1^ζ , the diffusion constant for the gate induced protein T_1 . In addition, transcribed proteins could alter – we know their first order quantitative effects due to our earlier analysis – $d_{pre,post}^\zeta$, the strength of the T_1 response, r , the fraction of T_1 free, g_p , the trigger gain, $[T_0]_b$, the trigger threshold concentration, s , the fraction of active T_1 reaching genome, g_e , the trigger gain for active T_1 transition, $[T_1]_n$, the threshold for T_1 , $[T_2]_n$, the threshold for $P(T_1) = T_2$, g_{T_2} , the gain for T_2 , ω , the feedback strength, and ξ , the feedback amount for $T_1 = 1 - \xi$.

The soma calculations are handled similar to what is outlined here.

6 The Abstract Neuron Output

We now understand in principle how to compute the axon hillock voltage that will be passed to the Hodgkin - Huxley engine to calculate the resulting action potential. The prime purpose of the incoming voltage is to provide the proper depolarization of the excitable cell membrane. Hence, we know that we will generate an action potential is the

incoming signal exceeds the neuron's threshold. For our purposes, the shape of the action potential will be primarily determined by the alteration of the g_{Na}^{Max} and g_K^{Max} conductance parameters. In our model, these values are altered by the second messenger triggers which create or destroy the potassium and sodium gates in the membrane. Other triggers alter the essential hardware of the neuron and potentially the entire neuron class \mathcal{N} in other ways. The protein T_2 due to a trigger u can have many effects.

6.1 The Hodgkin-Huxley Sodium and Potassium Model:

Hodgkin and Huxley modeled the sodium and potassium gates as

$$\begin{aligned} g_{Na}(V, t) &= g_0^{Na} m^3(V, t) h(V, t) \\ g_K(V, t) &= g_0^K n^4(V, t) \end{aligned}$$

where the two activation variables, m and n , and the one inactivation variable all satisfy first order kinetics of the form

$$\begin{aligned} \tau_m \frac{dm}{dt} &= m_\infty - m \\ \tau_h \frac{dh}{dt} &= h_\infty - h \\ \tau_n \frac{dn}{dt} &= n_\infty - n \end{aligned}$$

The time constants and asymptotes are defined to be

$$\begin{aligned} \tau_m &= \frac{1}{\alpha_m + \beta_m} \\ m_\infty &= \frac{\alpha_m}{\alpha_m + \beta_m} \\ \tau_h &= \frac{1}{\alpha_h + \beta_h} \\ h_\infty &= \frac{\alpha_h}{\alpha_h + \beta_h} \\ \tau_n &= \frac{1}{\alpha_n + \beta_n} \\ n_\infty &= \frac{\alpha_n}{\alpha_n + \beta_n}. \end{aligned}$$

Finally, the coefficient functions, α and β for each variable required data fits as functions of voltage. These were determined to be

$$\begin{aligned}
\alpha_m &= -0.10 \frac{V + 35.0}{e^{-.1(V+35.0)} - 1.0} \\
\beta_m &= 4.0 e^{\frac{-(V+60.0)}{18.0}} \\
\alpha_h &= 0.07 e^{-.05(V+60.0)} \\
\beta_h &= \frac{1.0}{(1.0 + e^{-.1(V+30.0)})} \\
\alpha_n &= -\frac{0.01 * (V + 50.0)}{(e^{-.1(V+50.0)} - 1.0)} \\
\beta_n &= 0.125 e^{-0.0125(V+60.0)}
\end{aligned}$$

In addition, we have the membrane voltage dynamics

$$\frac{dV}{dt} = \frac{I_M - I_K - I_{Na} - I_L}{C_M}$$

The resulting system is solved using initial conditions

$$\begin{aligned}
m(0) &= m_\infty(V_0, 0) \\
h(0) &= h_\infty(V_0, 0) \\
n(0) &= m_\infty(V_0, 0) \\
V(0) &= V_0
\end{aligned}$$

to determine the action potential which is emitted by the excitable cell. We note that at equilibrium there is no current across the membrane. Hence, the sodium and potassium currents are zero and the activation and inactivation variables should achieve their steady state values which would be m_∞ , h_∞ and n_∞ computed at the equilibrium membrane potential which is here denoted by V_0 . Then, under the voltage clamp protocol, we must solve,

$$\begin{aligned}
\frac{dV_m}{dt} &= \frac{1}{C_M} (I_K + I_{Na} + I_L - I_E) \\
&= \frac{1}{C_M} (g_{Na}(V, t)(V_m - E_K) + g_K(V, t)(V_m - E_{Na}) + g_L(V_m - E_L) - I_E) \\
&= (g_0^{Na} m^3(V, t) h(V, t) + g_0^K n^4(V, t) + g_L(V_m - E_L) - I_E)
\end{aligned}$$

using all the machinery of activation/ inactivation variables we have described.

6.1.1 Encoding The Dynamics:

Now these dynamics are more difficult to solve than you might think. The sequence of steps is this:

- Given the time t and voltage V compute

$$\begin{aligned}\alpha_m &= -0.10 \frac{V + 35.0}{e^{-.1(V+35.0)} - 1.0} \\ \beta_m &= 4.0 e^{\frac{-(V+60.0)}{18.0}} \\ \alpha_h &= 0.07 e^{-.05(V+60.0)} \\ \beta_h &= \frac{1.0}{(1.0 + e^{-.1(V+30.0)})} \\ \alpha_n &= -\frac{0.01 * (V + 50.0)}{(e^{-.1(V+50.0)} - 1.0)} \\ \beta_n &= 0.125 e^{-0.0125(V+60.0)}\end{aligned}$$

- Then compute the τ and steady state activation and inactivation variables

$$\begin{aligned}\tau_m &= \frac{1}{\alpha_m + \beta_m} \\ m_\infty &= \frac{\alpha_m}{\alpha_m + \beta_m} \\ \tau_h &= \frac{1}{\alpha_h + \beta_h} \\ h_\infty &= \frac{\alpha_h}{\alpha_h + \beta_h} \\ \tau_n &= \frac{1}{\alpha_n + \beta_n} \\ n_\infty &= \frac{\alpha_n}{\alpha_n + \beta_n}\end{aligned}$$

- Then compute the sodium and potassium potentials. In this model, this is easy as each is set only once since the internal and external ion concentrations always stay the same and so Nernst's equation only has to be used one time. Here we use the concentrations

$$[\text{Na}]_o = 491.0$$

$$[\text{Na}]_i = 50.0$$

$$[\text{K}]_o = 20.11$$

$$[\text{K}]_i = 400.0$$

These computations are also dependent on the temperature which is set to 9.3 degrees C.

- Next compute the conductances since we now know $m(V, t)$, $h(V, t)$ and $n(V, t)$.

$$g_{Na}(V, t) = g_0^{Na} m^3(V, t) h(V, t)$$

$$g_K(V, t) = g_0^K n^4(V, t)$$

Now here we will need the maximum sodium and potassium conductances g_0^{Na} and g_0^K to finish the computation. These values must be provided as data and in this model are not time dependent. Here we use

$$g_0^{Na} = 120.0$$

$$g_0^K = 36.0$$

- Then compute the ionic currents:

$$I_{Na} = g_{Na}(V, t)(V(t) - E_{Na})$$

$$I_K = g_K(V, t)(V(t) - E_K)$$

$$I_L = g_L(V, t)(V(t) - E_L)$$

where we use a value of the leakage conductance, g_L^0 , to be chosen later and a fixed leakage battery voltage.

$$g_L = g_L^0$$

$$E_L = -49.0$$

- Finally compute the total current

$$I_T = I_{Na} + I_K + I_L$$

- We can now compute the dynamics of our system at time t and voltage V : we let I_M denote the external current

to our system which we must supply.

$$\begin{aligned}\frac{dV}{dt} &= \frac{I_M - I_T}{C_M} \\ \frac{dm}{dt} &= \frac{m_\infty - m}{\tau_m} \\ \frac{dh}{dt} &= \frac{h_\infty - h}{\tau_h} \\ \frac{dn}{dt} &= \frac{n_\infty - n}{\tau_n}\end{aligned}$$

where we use $C_M = 1.0$.

The basic Hodgkin - Huxley model thus needs four independent variables which we place in a four dimensional vector y which components assigned as follows:

$$y = \begin{bmatrix} y[0] = V \\ y[1] = m \\ y[2] = h \\ y[3] = n \end{bmatrix}$$

We encode the dynamics calculated above into a four dimensional vector f whose components are interpreted as follows:

$$f = \begin{bmatrix} f[0] = \frac{I_M - I_T}{C_M} \\ f[1] = \frac{m_\infty - m}{\tau_m} \\ f[2] = \frac{h_\infty - h}{\tau_h} \\ f[3] = \frac{n_\infty - n}{\tau_n} \end{bmatrix}$$

which in terms of our vector y becomes

$$\begin{bmatrix} f[1] = \frac{m_\infty - y[1]}{\tau_m} \\ f[2] = \frac{h_\infty - y[2]}{\tau_h} \\ f[3] = \frac{n_\infty - y[3]}{\tau_n} \end{bmatrix}$$

So to summarize, at each time t and V , we need to calculate the four dimensional dynamics vector f for use in our choice of ODE solver. We can solve these equations for a typical external current pulse

$$I_E(t) = 1.0e^{-\frac{(t-0.2)^2}{0.1}} + 1.0e^{-\frac{(t-0.3)^2}{0.1}} + 1.0e^{-\frac{(t-0.4)^2}{0.1}} + 7.0e^{-\frac{(t-0.5)^2}{0.4}}$$

which we can see in Figure 8 injects a modest amount of current over approximately 2 seconds.

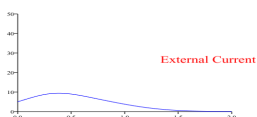
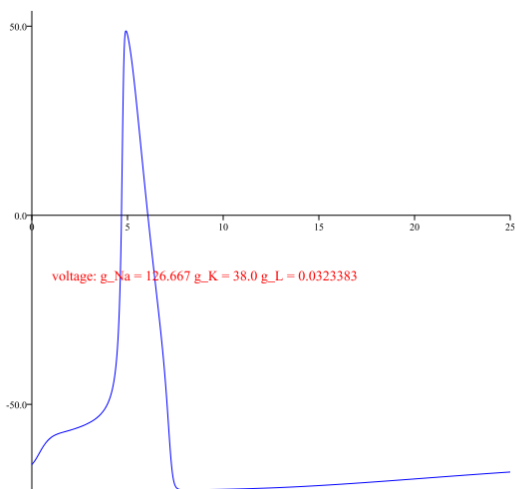
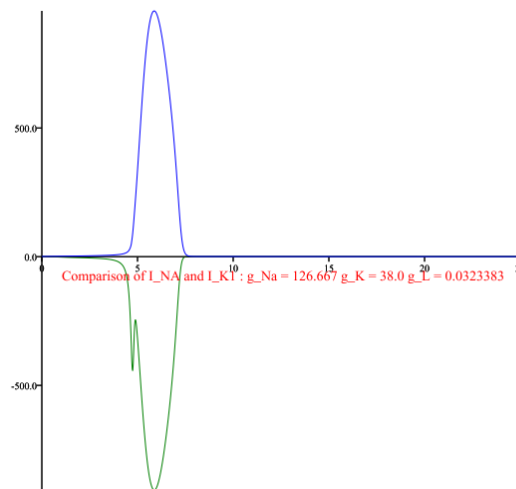


Figure 8: The Applied Synaptic Pulse

Let's examine how an action potential is generated with this model. We start with the excitation given by external current as shown in Figure 8. As this current flows into the membrane, the membrane begins to depolarize. The current flow of sodium and potassium through the membrane is voltage dependent and so this increase in the voltage across the membrane causes changes in the ion gates. In Figure 9(a), we see the voltage time trace and in Figure 9(b), we see the superimposed plots of sodium and potassium current on the right. Note how the potassium current lags the sodium current.



(a) Action Potential



(b) Simultaneous Sodium and Potassium Currents

Figure 9: The Action Potential And Ion Currents For A Pulse

Recall the ion current equations: The nonlinear conductance is modeled by

$$g_{Na}(V, t) = g_0^{Na} m^3(V, t) h(V, t)$$

$$g_K(V, t) = g_0^K n^4(V, t)$$

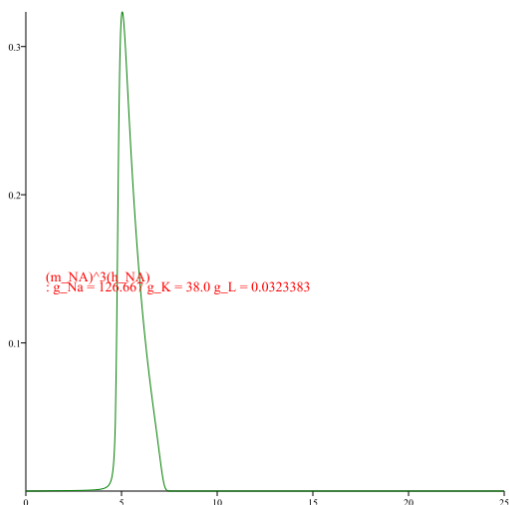
and the full current equations are

$$I_{Na} = g_{Na}(V, t)(V(t) - E_{NA})$$

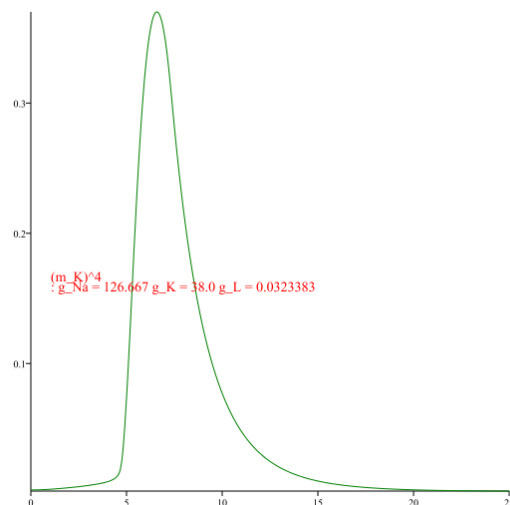
$$I_K = g_K(V, t)(V(t) - E_K)$$

$$I_L = g_L(V, t)(V(t) - E_L)$$

The conductance is in *micro Siemens* or units of 10^{-6} *1/ohms*. Time is in *milliseconds* or 10^{-3} *seconds* and voltage is in *millivolts* or 10^{-3} *volts*. The currents here are thus in units of 10^{-9} *amps* or *nano amps*. For our stated inner and outer sodium and potassium concentrations, our simulation uses the ion battery voltages $E_{NA} = 55.54$ mV and $E_K = -72.7004$ mV. Let's use $g_0^{Na} = 126.667$ and 38.0 for $g_0^K = 34.0$.



(a) The value of m^3h is shown for the pulse.



(b) The value of n^4 is shown for a pulse.

Figure 10: Sodium and Potassium Conductances

7 The Modulation of BFV Components:

We know that

$$C_m \frac{dV_M}{dt} = I_E - g_K^{Max} n^4(V_m, t)(V_m - E_K) - g_{Na}^{Max} m^3(V_m, t)h(V_m, t)(V_m - E_{Na}) - g_L(V_m - E_L).$$

Since the BFV is structured so that the action potential has a maximum at t_1 of value V_1 and a minimum at t_3 of value V_3 , we have $V'_m(t_1) = 0$ and $V'_m(t_3) = 0$. This gives

$$\begin{aligned} I_E(t_1) &= g_K^{Max} n^4(V_1, t_1)(V_1 - E_K) \\ &\quad + g_{Na}^{Max} m^3(V_1, t_1)h(V_1, t_1)(V_1 - E_{Na}) + g_L(V_1 - E_L) \\ I_E(t_3) &= g_K^{Max} n^4(V_3, t_3)(V_3 - E_K) \\ &\quad + g_{Na}^{Max} m^3(V_3, t_3)h(V_3, t_3)(V_3 - E_{Na}) + g_L(V_3 - E_L) \end{aligned}$$

From Figure 10(a) and Figure 10(b), we see that $m^3(V_1, t_1)h(V_1, t_1) \approx 0.35$ and $n^4(V_1, t_1) \approx 0.2$. Further, $m^3(V_3, t_3)h(V_3, t_3) \approx 0.01$ and $n^4(V_3, t_3) \approx 0.4$. Thus,

$$\begin{aligned} I_E(t_1) &= 0.20g_K^{Max}(V_1 - E_K) + 0.35g_{Na}^{Max}(V_1 - E_{Na}) + g_L(V_1 - E_L) \\ I_E(t_3) &= 0.40g_K^{Max}(V_3 - E_K) + 0.01g_{Na}^{Max}(V_3 - E_{Na}) + g_L(V_3 - E_L) \end{aligned}$$

Reorganizing,

$$\begin{aligned} I_E(t_1) &= (0.20g_K^{Max} + 0.35g_{Na}^{Max} + g_L)V_1 - (0.20g_K^{Max}E_K + 0.35g_{Na}^{Max}E_{Na} + g_LE_L) \\ I_E(t_3) &= (0.40g_K^{Max} + 0.01g_{Na}^{Max} + g_L)V_3 - (0.40g_K^{Max}E_K + 0.01g_{Na}^{Max}E_{Na} + g_LE_L) \end{aligned}$$

Solving for the voltages, we find

$$\begin{aligned} V_1 &= \frac{I_E(t_1) + 0.20g_K^{Max}E_K + 0.35g_{Na}^{Max}E_{Na} + g_LE_L}{0.20g_K^{Max} + 0.35g_{Na}^{Max} + g_L} \\ V_3 &= \frac{I_E(t_3) + 0.40g_K^{Max}E_K + 0.01g_{Na}^{Max}E_{Na} + g_LE_L}{0.40g_K^{Max} + 0.01g_{Na}^{Max} + g_L} \end{aligned}$$

Thus,

$$\frac{\partial V_1}{\partial g_K^{Max}} = 0.20E_K \frac{1}{0.20g_K^{Max} + 0.35g_{Na}^{Max} + g_L} + \frac{I_E(t_1) + 0.20g_K^{Max}E_K + 0.35g_{Na}^{Max}E_{Na} + g_LE_L}{0.20g_K^{Max} + 0.35g_{Na}^{Max} + g_L} \frac{-1.0}{0.20g_K^{Max} + 0.35g_{Na}^{Max} + g_L} .20$$

This simplifies to

$$\frac{\partial V_1}{\partial g_K^{Max}} = \frac{0.20}{0.20g_K^{Max} + 0.35g_{Na}^{Max} + g_L} (E_K - V_1) \quad (44)$$

Similarly, we find

$$\frac{\partial V_1}{\partial g_{Na}^{Max}} = \frac{0.35}{0.20g_K^{Max} + 0.35g_{Na}^{Max} + g_L} (E_{Na} - V_1) \quad (45)$$

$$\frac{\partial V_3}{\partial g_K^{Max}} = \frac{0.40}{0.40g_K^{Max} + 0.01g_{Na}^{Max} + g_L} (E_K - V_3) \quad (46)$$

$$\frac{\partial V_3}{\partial g_{Na}^{Max}} = \frac{0.40}{0.40g_K^{Max} + 0.01g_{Na}^{Max} + g_L} (E_{Na} - V_3) \quad (47)$$

We also know that as t goes to infinity, the action potential flattens and V'_m approaches 0. Also, the applied current, I_E is zero and so we must have

$$0 = -g_K^{Max}n^4(V_\infty, \infty)(V_\infty - E_K) - g_{Na}^{Max}m^3(V_\infty, \infty)h(V_\infty, \infty)(V_\infty - E_{Na}) - g_L(V_\infty - E_L)$$

Our hyperpolarization model is

$$Y(t) = V_3 + (V_4 - V_3) \tanh(g(t - t_3))$$

We have V_∞ is V_4 . Thus,

$$0 = -g_K^{Max}n^4(V_4, \infty)(V_4 - E_K) - g_{Na}^{Max}m^3(V_4, \infty)h(V_4, \infty)(V_4 - E_{Na}) - g_L(V_4 - E_L)$$

This gives, letting $m^3(V_4, \infty)h(V_4, \infty)$ and $n^4(V_4, \infty)$ be denoted by $(m^3h)^*$ and $(n^4)^*$ for simplicity of exposition,

$$(g_K^{Max}(n^4)^* + g_{Na}^{Max}(m^3h)^* + g_L)V_4 = (g_K^{Max}(n^4)^*E_K + g_{Na}^{Max}(m^3h)^*E_{Na} + g_LE_L)$$

Hence,

$$V_4 = \frac{g_K^{Max}n^4(V_4, \infty)E_K + g_{Na}^{Max}m^3(V_4, \infty)h(V_4, \infty)E_{Na} + g_LE_L}{g_K^{Max}n^4(V_4, \infty) + g_{Na}^{Max}m^3(V_4, \infty)h(V_4, \infty) + g_L}$$

We see

$$\frac{\partial V_4}{\partial G_K^{Max}} = \frac{n^4(V_4, \infty)}{g_K^{Max}n^4(V_4, \infty) + g_{Na}^{Max}m^3(V_4, \infty)h(V_4, \infty) + g_L} (E_K - V_4) \quad (48)$$

$$\frac{\partial V_4}{\partial G_{Na}^{Max}} = \frac{m^3(V_4, \infty)h(V_4, \infty)}{g_K^{Max}n^4(V_4, \infty) + g_{Na}^{Max}m^3(V_4, \infty)h(V_4, \infty) + g_L} (E_{Na} - V_4) \quad (49)$$

We can also assume that the area under the action potential curve from the point (t_0, V_0) to (t_1, V_1) is proportional to the incoming current applied. If V_{In} is the axon - hillock voltage, the impulse current applied to the axon - hillock is $g_{In}V_{In}$ where g_{In} is the ball stick model conductance for the soma. Thus, the approximate area under the action potential curve must match this applied current. We have

$$\frac{1}{2} (t_1 - t_0) (V_1 - V_0) \approx g_{In}V_{In}$$

We conclude

$$(t_1 - t_0) = \frac{2g_{In}V_{In}}{V_1 - V_0}$$

Thus

$$\frac{\partial t_1 - t_0}{\partial g_K^{Max}} = -\frac{t_1 - t_0}{V_1 - V_0} \frac{\partial V_1}{\partial G_K^{Max}} \quad (50)$$

$$\frac{\partial t_1 - t_0}{\partial g_{Na}^{Max}} = -\frac{t_1 - t_0}{V_1 - V_0} \frac{\partial V_1}{\partial G_{Na}^{Max}} \quad (51)$$

$$(52)$$

Also, we know that during the hyperpolarization phase, the sodium current is off and the potassium current is slowly bringing the membrane potential back to the reference voltage. Now, our BFV model does not assume that the membrane potential returns to the reference level. Instead, by using

$$Y(t) = V_3 + (V_4 - V_3) \tanh(g(t - t_3))$$

we assume the return is to voltage level V_4 . At the midpoint, $Y = \frac{1}{2}(V_3 + V_4)$, we find

$$\frac{1}{2}(V_4 - V_3) = (V_4 - V_3) \tanh(g(t - t_3))$$

Thus, letting $u = g(t - t_3)$,

$$\frac{1}{2} = \frac{e^{2u} - 1}{e^{2u} + 1}$$

and we find $u = \frac{\ln(3)}{2}$. Solving for t , we then have

$$t^* = t_3 + \frac{\ln(3)}{2g}$$

From t_3 on, the Hodgkin - Huxley dynamics are

$$C_m \frac{dV_M}{dt} = -g_K^{Max} n^4(V_m, t)(V_m - E_K) - g_L(V_m - E_L).$$

We want the values of the derivatives to match at t^* . This gives

$$g(V^* - V_3) \operatorname{sech}^2[g(t^* - t_3)] = -\frac{g_K^{Max}}{C_m} n^4(V^*, t^*)(V^* - E_K) - g_L(V^* - E_L)$$

where $V^* = (V_3 + V_4)$. Now $g(t^* - t_3) = \frac{\ln(3)}{2}$ and thus we find

$$g \frac{1}{2} (V_4 - V_3) \operatorname{sech}^2[g(t^* - t_3)] = -\frac{g_K^{Max}}{C_m} n^4(V^*, t^*)(V^* - E_K) - \frac{g_L}{C_m} (V^* - E_L)$$

$$g \frac{1}{2} (V_4 - V_3) \frac{9}{64} = -\frac{g_K^{Max}}{C_m} n^4 (V^*, t^*) (V^* - E_K) - g_L (V^* - E_L)$$

Next, consider the magnitude of $n^4(V^*, t^*)$. We know at t^* , n^4 is small from Figure 10(b). Thus, we will replace it by the value 0.01. This gives

$$g \frac{1}{2} (V_4 - V_3) \frac{9}{64} = -0.01 \frac{g_K^{Max}}{C_m} \left(\frac{1}{2} (V_4 + V_3) - E_K \right) - \frac{g_L}{C_m} \left(\frac{1}{2} (V_4 + V_3) - E_L \right)$$

Simplifying, we have

$$\begin{aligned} \frac{9g}{128} (V_4 - V_3) &= (0.01 \frac{g_K^{Max}}{C_m} E_K + \frac{g_L}{C_m} E_L) - \frac{1}{2} (0.01 \frac{g_K^{Max}}{C_m} + \frac{g_L}{C_m}) (V_4 + V_3) \\ \frac{9g}{64} &= (0.01 \frac{g_K^{Max}}{C_m} E_K + \frac{g_L}{C_m} E_L) \frac{1}{V_4 - V_3} - (0.01 \frac{g_K^{Max}}{C_m} + \frac{g_L}{C_m}) \frac{V_4 + V_3}{V_4 - V_3} \end{aligned}$$

We can see clearly from the above equation, that the dependence of g on g_K^{Max} and g_{Na}^{Max} is quite complicated. However, we can estimate this dependence as follows. We know that $V_3 + V_4$ is about the reference voltage, $-65.9mV$. If we approximate V_3 by the potassium battery voltage, $E_K = -72.7mV$ and V_4 by the reference voltage, we find $\frac{V_3 + V_4}{V_4 - V_3} \approx \frac{-138.6}{6.8} = -20.38$ and $\frac{1}{V_4 - V_3} \approx \frac{1}{6.8} = 0.147$. Hence,

$$\begin{aligned} \frac{9C_m g}{64} &= 0.147(0.01g_K^{Max} E_K + g_L E_L) + 20.38(0.01g_K^{Max} + g_L) \\ &= (0.0147E_K + 2.038E_L)g_K^{Max} + g_L(0.0147E_L + 20.38) \end{aligned}$$

Thus, we find

$$\frac{\partial g}{\partial g_K^{Max}} = \frac{64}{9C_m} (0.0147E_K + 2.038E_L) \quad (53)$$

This gives $\frac{\partial g}{\partial g_K^{Max}} \approx -710.1$

Equation 53 shows what our intuition tells us: if g_K^{Max} increases, the potassium current is stronger and the hyperpolarization phase is shortened. On the other hand, if g_K^{Max} decreases, the potassium current is weaker and the hyperpolarization phase is lengthened.

8 Conclusions:

We now understand in principle how to modulate the components of the low dimensional feature vector, BFV, due to first and second messenger effects which arrive at the dendritic and soma modules of the neuron. For many purposes, the shape of the action potential will be primarily determined by the alteration of the g_{Na}^{Max} and g_K^{Max} conductance parameters which are altered by the second messenger triggers which create or destroy the potassium and sodium gates in the membrane. Other triggers alter the essential hardware of the neuron and potentially the entire neuron class \mathcal{N} in other ways. The protein T_2 due to a trigger u can

- directly alter the synaptic coupling weight $c_{pre, post}^u$ according to the strength of $T_2(t, w)$ by making changes in the extracellular side of the membrane in a variety of ways,
- can directly impact the maximum conductances for the potassium and sodium ions,
- can alter second messenger channels in many ways as we have discussed in the chapters on calcium and generic second messenger triggers. These alterations can affect the coupling weight or maximum ion conductances as well.

However, they can also effect more global parameters. Consider if the protein alters the ration ρ . This is a fundamental coupling parameter for the dendrite and soma system we use in our modeling. Hence, an alteration in ρ is a global change to the entire neuron class \mathcal{N} . This mechanism is very useful as it allows us to use monoamine modulation to alter every neuron in a particular class no matter what neural module it is a part of. This is a useful tool in implementing true RF type core modulation of cortical output. Such a global change could be as simple as an alteration to L_{DE} or L_{SE} without changing ρ . However, if ρ is changed to $\rho \pm \epsilon$, this changes the eigenvalue problem that the neuron class is associated with to

$$\tan(\alpha L) = -\frac{\tanh(L)}{(\rho \pm \epsilon)L}(\alpha L),$$

This paper leaves out many of the details of these matters. However, our complete derivations, motivations and computational details can found in (Peterson (6) 2005) .

This paper is only part of the story of course. The algorithms to compute axon hillock voltages, with all of their influences due to second messenger effects, have been outlined in (Peterson (5) 2005) . They and the BFV modulation algorithms discussed in this paper have been carefully designed to be implementable within an asynchronous computing environment using the Twisted Python package (Twi (9) 2004) . Once an axon hillock voltage is presented to the Hodgkin - Huxley action potential machinery, a BFV will be generated if threshold is surpassed. The details of how the BFV is modulated by the axon hillock voltage, the sodium and potassium maximum conductance changes and neurotransmitters are what have been described in this paper. The implementation details in Python are ongoing

and these abstract neural elements are being used to develop asynchronous software architectures for system level neural modeling. Of particular interest to us is the potential use of these ideas in the modeling of depression and other cognitive dysfunctions. These illnesses require the ability to use co-modulation of neurotransmitter gates. Our efforts here provide a solid foundation for neural elements which will support such co-modulation.

9 Acknowledgments:

We are grateful to the Air Force Research Laboratory for providing an interesting environment in which to work during the Summer of 2005 on issues of cognitive modeling.

10 References

References

- [1] Z. Hall. *An Introduction to Molecular Neurobiology*. Sinauer Associates Inc., Sunderland, MA, 1992.
- [2] A. Hodgkin. The Components of Membrane Conductance in the Giant Axon of Loligo. *J. Physiol. (London)*, 116: 473 – 496, 1952.
- [3] A. Hodgkin. The Ionic Basis of Electrical Activity in Nerve and Muscle. *Bio. Rev.*, 26:339 – 409, 1954.
- [4] A. Hodgkin and A. Huxley. Currents Carried by Sodium and Potassium Ions Through the Membrane of the Giant Axon of Loligo. *J. Physiol. (London)*, 116:449 – 472, 1952.
- [5] J. Peterson. Abstract second messenger objects and excitable cell input integration. *Journal Of Theoretical Medicine*, pages Manuscript: 1 – 48, 2005. submitted July 31, 2005.
- [6] J. Peterson. *A Primer on Cognitive Modeling*. www.ces.clemson.edu/~petersj/Books/BioComputation.pdf, 2005.
- [7] J. Peterson and T. Khan. Abstract action potential models for toxin recognition. *Journal Of Theoretical Medicine*, pages Manuscript: 1 – 32, 2005-1. submitted October 13, 2005.
- [8] F. Prete, editor. *Complex Worlds from Simpler Nervous Systems*. MIT Press, 2004. A Bradford Book.
- [9] *Twisted*. Twisted Matrix Laboratories, twistedmatrix.com, 2004. Version 1.3.0-1.1.